Hydrogeologic Setting and Preliminary Data Analysis for the Hydrologic-Budget Assessment of Lake Barco, an Acidic Seepage Lake in Putnam County, Florida

By L.A. Sacks, T.M. Lee, and A.B. Tihansky

U.S. GEOLOGICAL SURVEY
Water-Resources Investigations Report 91–4180

Prepared in cooperation with the
FLORIDA DEPARTMENT OF ENVIRONMENTAL REGULATION

Tallahassee, Florida
1992

U.S. DEPARTMENT OF THE INTERIOR
MANUEL LUJAN, JR., Secretary

U.S. GEOLOGICAL SURVEY
DALLAS L. PECK, Director

For additional information,
write to:

District Chief
U.S. Geological Survey
Suite 3015
227 North Bronough Street
Tallahassee, Florida 32301

Copies of this report may be
purchased from:

U.S. Geological Survey
Books and Open-File Reports Section
Federal Center
Box 25425
Denver, Colorado 80225

CONTENTS

Conversion Factors, Vertical Datum, Acronyms, and Additional Abbreviations

Multiply	By	To obtain
inch (in.)	25.4	millimeter
foot (ft)	0.3048	meter
mile (mi)	1.609	kilometer
mile per hour (mi/h)	1.609	kilometer per hour
acre	0.4047	hectare
cubic foot (ft^3)	0.02832	cubic meter

Temperature in degrees Fahrenheit (°F) can be converted to degrees Celsius (°C) as follows: $°C = 5/9\ (°F - 32)$

Sea level: In this report, "sea level" refers to the National Geodetic Vertical Datum of 1929 (NGVD of 1929)—a geodetic datum derived from a general adjustment of the first-order level nets of the United States and Canada, formerly called Sea Level Datum of 1929.

Acronyms used in report:

ANC	acid neutralizing capacity
GPR	ground-penetrating radar
NOAA	National Oceanic and Atmospheric Administration
PAR	photosynthetically active radiation

Additional abbreviations used in report:

$(cal/cm^2)/d$	calories per square centimeter per day
cm	centimeter
R^2	coefficient of determination
$(Ei/m^2)/d$	Einsteins per square meter per day
Hz	hertz
J	joule
m	meter
m/s	meters per second
µeq/L	microequivalents per liter
µS/cm	microsiemens per centimeter at 25 degrees Celsius
mb	millibars
mm/yr	millimeters per year
$(mJ/m^2)/d$	millijoules per square meter per day
nm	nanometers
s	seconds

NOTE: Inch-pound units were selected for use in this report. An exception to the use of inch-pound units, however, is made in the presentation of data collected for the energy budget and mass-transfer evaporation methods. The metric unit of calories per square centimeter is conventionally used to describe the energy terms in an energy budget analysis (Anderson, 1954; Sturrock, 1985). Temperatures used in the computation of energy terms have been left in the compatible metric unit of degrees Celsius. The mixed units that are conventionally used to describe the components of the mass-transfer evaporation method (Harbeck, 1962; Sturrock, 1985) also are used in this report.

Hydrogeologic Setting and Preliminary Data Analysis for the Hydrologic-Budget Assessment of Lake Barco, an Acidic Seepage Lake in Putnam County, Florida

By L.A. Sacks, T.M. Lee, *and* A.B. Tihansky

Abstract

Lake Barco is an acidic seepage lake in north-central Florida. To better understand the mechanisms controlling the acid neutralizing capacity in the lake, a study was initiated to quantify the hydrologic and solute budgets of the lake. Geologic data were evaluated to determine the local hydrogeology and the structural framework of the lake. Climatic and hydrologic data that were required to determine the hydrologic budget of Lake Barco were collected between May 1989 and December 1990. These data include daily climatic variables for computing lake evaporation by the energy-budget and mass-transfer methods. Lake stage and the vertical and areal hydraulic head distribution in the aquifers around the lake were measured starting in September 1988 and were used to describe the ground-water flow patterns around Lake Barco.

Lithologic data and results of surface geophysical techniques indicate that Lake Barco probably is the surficial expression of a sinkhole. The local basin is underlain by 100 to 150 feet of unconsolidated sands and clays, with differential settling into karst solution features in the underlying limestone. The surficial aquifer system and lake are in the unconsolidated surficial deposits, and recharge to the underlying Upper Floridan aquifer is by downward leakage through the intermediate confining unit. The downward head difference between the lake and the Upper Floridan aquifer is about 5 feet. Lake Barco is a flow-through lake with respect to the surficial aquifer system. During the period of data collection, ground-water inflow occurred along the northeastern perimeter of the lake and outflow occurred along the southern perimeter. During the fall and early winter of 1988, ground-water inflow also occurred along the northwestern perimeter of the lake following a period of high recharge. Outflow from the lake is southward toward an area of lower heads. These lower head values in the surficial aquifer system may be controlled by a better hydraulic connection between the surficial aquifer system and the Upper Floridan aquifer.

Climatic and hydrologic data collected during this study reflect drier than average conditions. Rainfall during the 20-month period of data collection (May 1989-December 1990) was 72.12 inches, almost 20 inches below the long-term mean in Gainesville. As a result, lake stage declined from a high of 88.02 feet above sea level in December 1988 to a low of 81.19 feet above sea level on January 1, 1991. Lake volume was reduced by 45 percent during this period. Ground-water heads also declined by amounts similar to lake-stage declines. Daily mean lake temperature ranged from 8.9 to 32.8 degrees Celsius, and daily mean air temperature ranged from -4.0 to 30.0 degrees Celsius. The lake does not seasonally stratify, and daily mean lake temperature generally varied by less than 1 degree Celsius from the surface to the bottom of the lake. Daily mean vapor pressure of the air ranged from 4.4 to 32.0 millibars.

INTRODUCTION

Florida has the highest number of acidic lakes in the United States according to results of a national survey by the U.S. Environmental Protection Agency (Landers and others, 1988). Most of these lakes are seepage lakes that have no surface-water inlets or outlets. Permeable, sandy soils prevent significant runoff from the drainage basins. As a result, ground-water inflow and precipitation on the lake surface are the primary sources of water for these lakes. Because precipitation is a dominant component of their hydrologic budgets, these lakes may be vulnerable to increases in acidic deposition due to their low acid neutralizing capacity (ANC) (Eilers and others, 1988).

A number of factors regulate the ANC in acidic lakes, including the hydrologic regime of the lake, in-lake biogeochemical processes that generate or consume ANC, and the chemical fluxes to the lake from atmospheric deposition and ground water (Baker and Brezonik, 1988). Although the factors that regulate ANC are recognized, the relative importance of each is not known. For example, ground-water inflow may contribute a significant fraction of the lake water ANC, even though it may be a small component of the hydrologic budget of the lakes (Baker and others, 1988). In addition, the long-term effect of changes in processes regulating ANC on lake chemistry is not understood.

A detailed hydrologic budget is fundamental to understanding the factors that regulate lake water ANC. The budget is a prerequisite to quantifying chemical fluxes to the lake and the effects of evaporative concentration of chemicals in the lake. The hydrologic budget should accurately quantify, over a given time period, all water fluxes to and from the lake (precipitation, evaporation, ground-water inflow, and leakage), change in lake storage, and the uncertainty associated with measuring each of these quantities. Of these budget terms, evaporative losses and ground-water fluxes (inflow and leakage) are the most difficult to quantify. By using the best available methods, uncertainty in monthly estimates of evaporation can be as little as 10 percent, whereas estimates of ground-water fluxes can contain errors on the order of 100 percent (Winter, 1981; Wentz and others, 1989; T.M. Lee and Amy Swancar, U.S. Geological Survey, written commun., 1990). This large uncertainty reflects the difficulty of accurately defining hydrogeologic properties of the ground-water basins surrounding lakes.

In 1988, the U.S. Geological Survey, in cooperation with the Florida Department of Environmental Regulation, began a 4-year study of the factors influencing the ANC in Lake Barco, an acidic seepage lake in north-central Florida. Detailed hydrologic and chemical budgets were needed to provide the basis for understanding ANC fluxes to the lake (Pollman and others, 1991). To define the hydrologic budget, numerous hydrologic and climatologic variables were monitored over a 20-month period from May 1989 through December 1990. Hydrogeologic data also were collected to define the geometry and physical properties of the aquifers that surround the lake. This information is critical for accurately interpreting ground-water fluxes to the lake. To define the chemical budget of the lake, the chemical composition of atmospheric deposition, lake water, ground water, and the porewater in the lake sediments also were monitored for this same period.

Purpose and Scope

This report has two objectives: to describe the hydrogeologic setting of Lake Barco and to summarize a preliminary analysis of data collected for the computation of the hydrologic budget of the lake. Data are described that will be used to compute terms of the hydrologic budget of the lake. These terms include lake storage, precipitation, evaporation, ground-water inflow, and leakage. Overland flow is considered to be negligible and is not being quantified. Precipitation and other climatological data are presented for April 28, 1989, through January 2, 1991. Lake stage and ground-water level data for the drainage basin are presented for a longer period, from late September 1988 through early January 1991. To further understand ground-water flow patterns around the lake, the hydrogeologic setting of the lake is described. The hydrogeologic setting described in this report includes basin stratigraphy as determined from well-drilling logs and natural gamma borehole logs. Sublake geology was defined by sediment thickness measurements, ground-penetrating radar, and seismic reflection.

Description of Study Site

Lake Barco is an acidic seepage lake in western Putnam County, Fla., approximately 2.5 mi southeast of Melrose, 20 mi east of Gainesville, and 20 mi west of Palatka (fig. 1). The surface area of Lake Barco is 29 acres, mean depth is 13 ft, and maximum depth is 22 ft at a stage of 87.6 ft above sea level. The lake bottom has a fairly steep slope around the perimeter of the lake, whereas the center of the lake is predominantly flat (fig. 2). The lake is extremely clear, and light penetration allows submerged vegetation to grow over most of the lake bottom. In May 1989, the lake pH was 4.5, specific conductance was 42 µS/cm, and ANC was -36 µeq/L.

Lake Barco and its topographic basin lie entirely within the Katharine Ordway Preserve (fig. 3), a 10,000-acre tract of sandhills, lakes, and cypress swamp owned by the Nature Conservancy and managed by the University of Florida. To the north of Lake Barco, a ridge rises to an altitude of 160 ft above sea level (approximately 70 ft above lake stage). The topography is considerably more flat to the south, and land surface generally is less than 100 ft above sea level. Three lakes are less than 0.5 mi from Lake Barco: Lake Rowan to the west, Lake Goodson to the south, and Long Lake to the southeast (fig. 4). Vegetation in the upland areas consists predominantly of longleaf pine *(Pinus palustris)* with an understory of turkey oak *(Quercus laevis)*. Live oak *(Quercus geminata)* and slash pine *(Pinus elloittii)* are found closer to the lake. The woody shrub, St.-Johnswort *(Hypericum fasciculatum)*, forms a ring immediately adjacent to the lake (Franz and Hall, 1990).

The climate in north-central Florida is humid subtropical. Mean annual rainfall (1951-80) is 52.84 in. at the National Oceanic and Atmospheric Administration (NOAA) 3WSW site in Gainesville (National Oceanic and Atmospheric Administration, 1988). Most of the rain occurs in the summer months and is associated with afternoon and evening thunderstorms. Rainfall from winter frontal activity generally is not as intense as the summer storms.

Acknowledgments

The authors are grateful to the Advisory Board of the Katharine Ordway Preserve for permission to work within the preserve and to the preserve caretaker, Truman Perry, for his help with the logistics of drilling wells on the preserve. We also appreciate the assistance of Ingrid Prentice, who maintained and operated the land-based climate station and

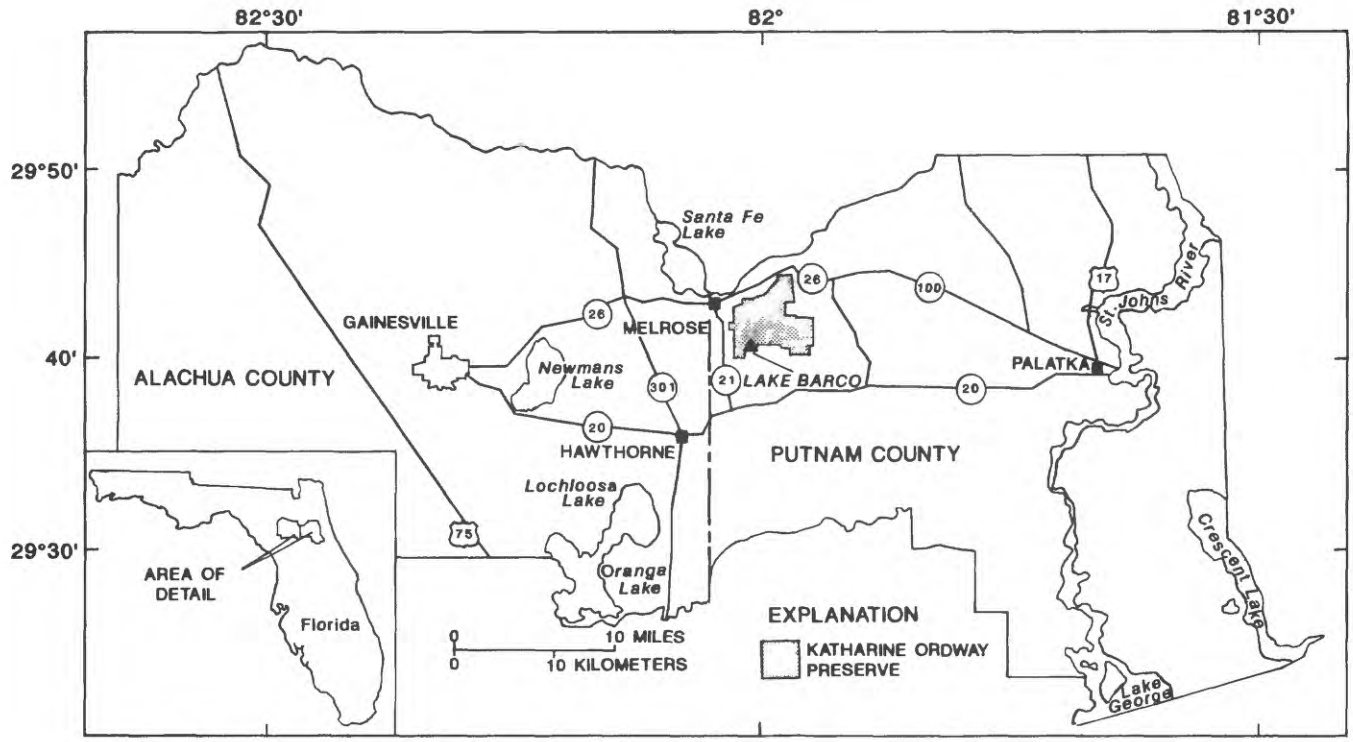

Figure 1. Location of the study site.

monitored ground-water levels and lake levels around Lake Barco; and Millard Fisher, who maintained the raft-based climate station and performed lake thermal surveys.

GEOLOGIC DESCRIPTION

Lake Barco lies within the Interlachen Sand Hills part of the Central Lake physiographic district (Brooks, 1981). The Central Lake District, which runs along the central part of the Florida Peninsula, is a region of active sinkhole development. Unconsolidated sediments fill solution voids in the underlying limestone, which results in surficial depressions and lakes (Lane, 1986). Many of the numerous lakes in this region are believed to be cover-collapse sinkholes that are surficial expressions of underlying karst features (Sinclair and Stewart, 1985; Arrington and Lindquist, 1987). Surface topography is controlled by sandhill or mantled karst. A direct hydraulic connection exists between the overlying thick sand and gravel deposits and the underlying carbonate rocks within much of the Interlachen Sand Hills region (Brooks, 1981).

General Hydrogeology

The hydrogeologic units of interest in this report (table 1) are those that influence ground-water interactions with the lake. The surficial aquifer system occurs within undifferentiated surficial deposits of Holocene to Pliocene age. These deposits generally consist of clayey sands to sandy clays and are found from land surface to depths of about 50 to 100 ft (Bermes and others, 1963). Below the surficial aquifer system is the intermediate confining unit that separates the surficial aquifer system from the Floridan aquifer system (Southeastern Geological Society, 1986). This unit encompasses the

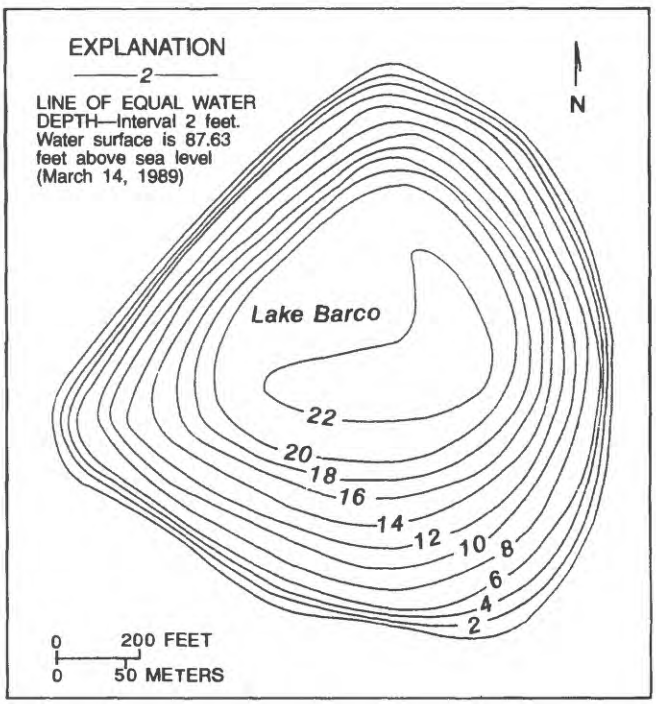

Figure 2. Bathymetry of Lake Barco.

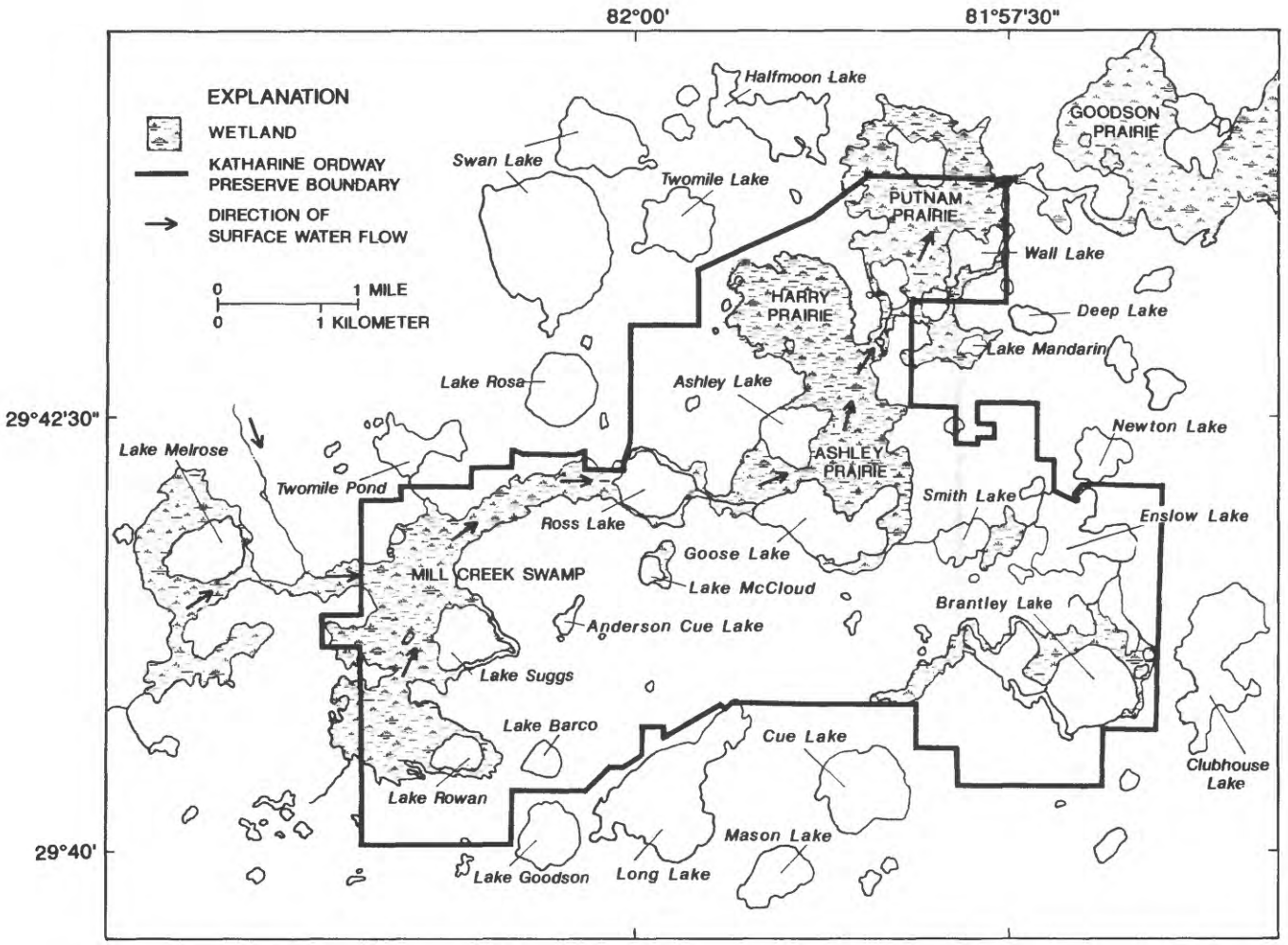

Figure 3. Lakes within and near the Katharine Ordway Preserve. (Modified from Franz and Hall, 1990.)

Hawthorn Group of Miocene age, which is approximately 50 to 100 ft thick and is composed of a varied mixture of sand, gravel, clay, phosphate, and carbonate (Scott, 1983). (Stratigraphic nomenclature in this report is that of the Florida Geological Survey and does not necessarily follow usage of the U.S. Geological Survey.) Although considered a confining unit, permeable beds of localized extent do occur within the Hawthorn Group. In addition, karst features in the underlying limestone can cause disruptions in overlying confining units. These breaks in the intermediate confining unit can result in a more direct hydraulic connection between the surficial aquifer system and the Floridan aquifer system (Sinclair and Stewart, 1985; Miller, 1986; Aucott, 1988).

The Floridan aquifer system is a vertically continuous sequence of carbonate rocks of high permeability and regional extent (Miller, 1986). The uppermost part of the Floridan aquifer system, called the Upper Floridan aquifer, occurs in the Ocala Group of Upper Eocene age. This unit consists of an approximately 200-ft-thick sequence of limestone and dolomite and is the principal water-bearing zone in western Putnam County (Bermes and others, 1963). Downward hydraulic gradients dominate between the principal hydrogeologic units, making this region an important recharge area to the Upper Floridan aquifer (Yobbi and Chappell, 1979; Stewart, 1980; Aucott, 1988).

Basin Stratigraphy

Geologic information was collected when observation wells were installed in the Lake Barco basin to monitor vertical and areal hydraulic-head distribution. The wells fall into two categories: water-table wells and nested wells. The nested wells were finished at various depths between the water table in the surficial aquifer system and the top of the Upper Floridan aquifer. Water-table wells (fig. 5) were finished approximately 5 ft below the water table. Information on the deeper geology was obtained from nested wells at three sites near the lake (fig. 5). Split-spoon cores were collected from an additional test hole near one of the well nests (site SS). Table 2 provides a description of well characteristics.

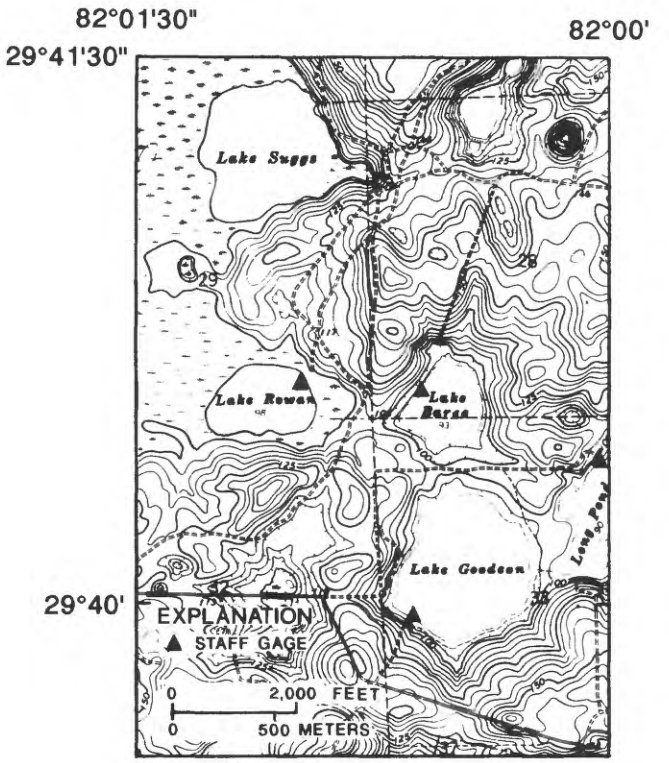

Figure 4. Topography of the study area and location of staff gages.

Samples of the surficial deposits near Lake Barco consist mainly of sand, silt to clay-rich sands, and sandy clays, ranging in color from light brown to blue-gray to light orange. In the southern part of the basin, the deposits are generally more clay-rich than in the northern part. At the nested well sites near the lake, the surficial deposits range in thickness from 33 to 53 ft. In upper parts of the basin, where land surface is up to 50 ft higher, the thickness of the surficial deposits may be considerably greater.

The contact between the surficial deposits and the Hawthorn Group is not readily apparent from drilling logs. Generally, there is a gradation to increasing amounts of clay and phosphate and a color change to olive-green and gray-blue. The contact is better defined by natural gamma geophysical logs because the Hawthorn Group has significantly higher gamma radiation than do the surficial deposits (Scott, 1988). Uranium-bearing phosphate minerals that occur throughout the Hawthorn Group account for the increased gamma activity. A natural gamma geophysical log was completed in the deepest well at each of the three well nests. These logs indicate that the top of the Hawthorn Group occurs at altitudes of 45, 60, and 52 ft above sea level at sites 1PNB, 2PNB, and 3PNB, respectively (fig. 6). The Hawthorn deposits are generally poorly sorted sandy clays to clayey sands, with coarser fractions of quartz and phosphate. Clay mineralogy was not determined, but according to Reik (1982), the most common clays in the Hawthorn Group in northeastern Florida are palygorskite and montmorillonite. Sharks' teeth and shell fragments occur in several beds.

Table 1. Relation of stratigraphic and hydrogeologic units at the study site

Age	Stratigraphic unit	Hydrogeologic unit	Physical description	Near Lake Barco	
				Unit thickness (range in feet)	Altitude of top of unit (range in feet)
Holocene to Pliocene	Undifferentiated surficial deposits	Surficial aquifer system	Sand, clayey sand, and sandy clay.	[1]33 to 53	98 to 93 (land surface)
Miocene	Hawthorn Group[2]	Intermediate confining unit	Phosphatic, poorly sorted sandy clay, clayey sand, and gravel.	[1]57 to 98	60 to 45
Upper Eocene	Ocala Group[2]	Upper Floridan aquifer	Porous, white, fossiliferous limestone; dolomitic beds in lower part.	[3]200	-3 to -46

[1]Determined from well nests 1PNB, 2PNB, and 3PNB. Units may be thicker in parts of the basin where land surface is higher.

[2]Southeastern Geological Society (1986).

[3]Bermes and others (1963).

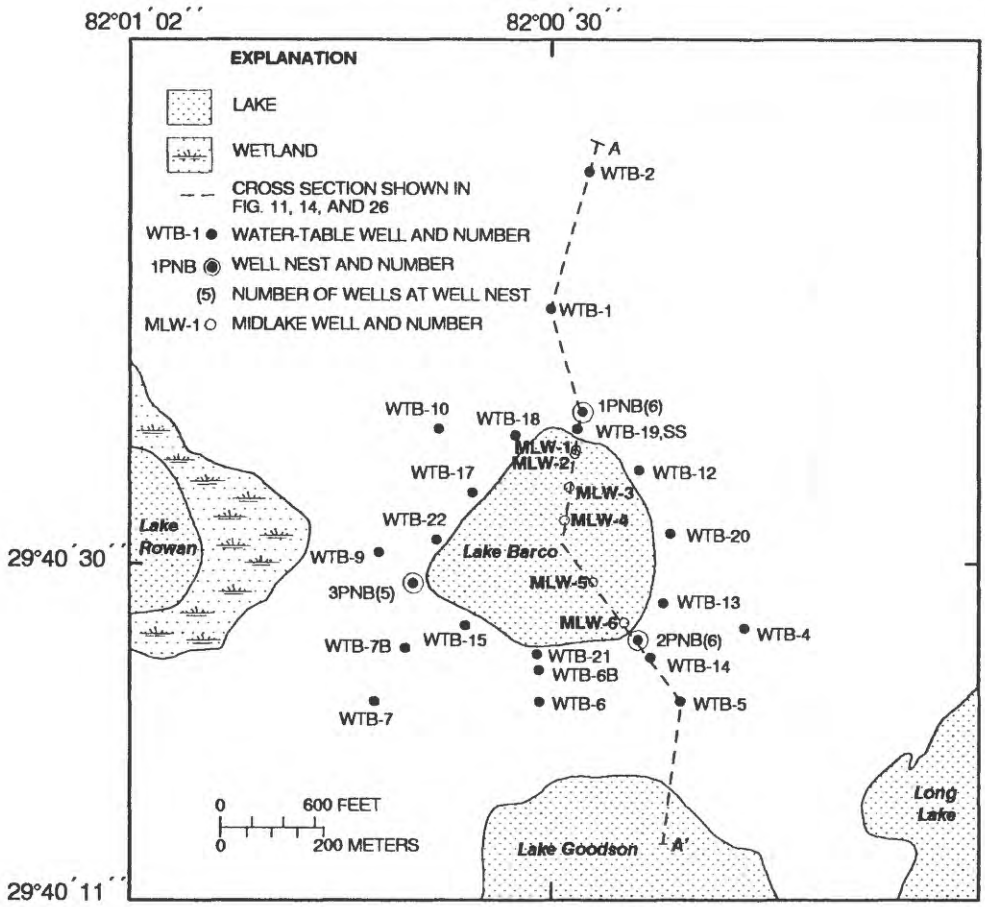

Figure 5. Location of monitoring wells around and in Lake Barco.

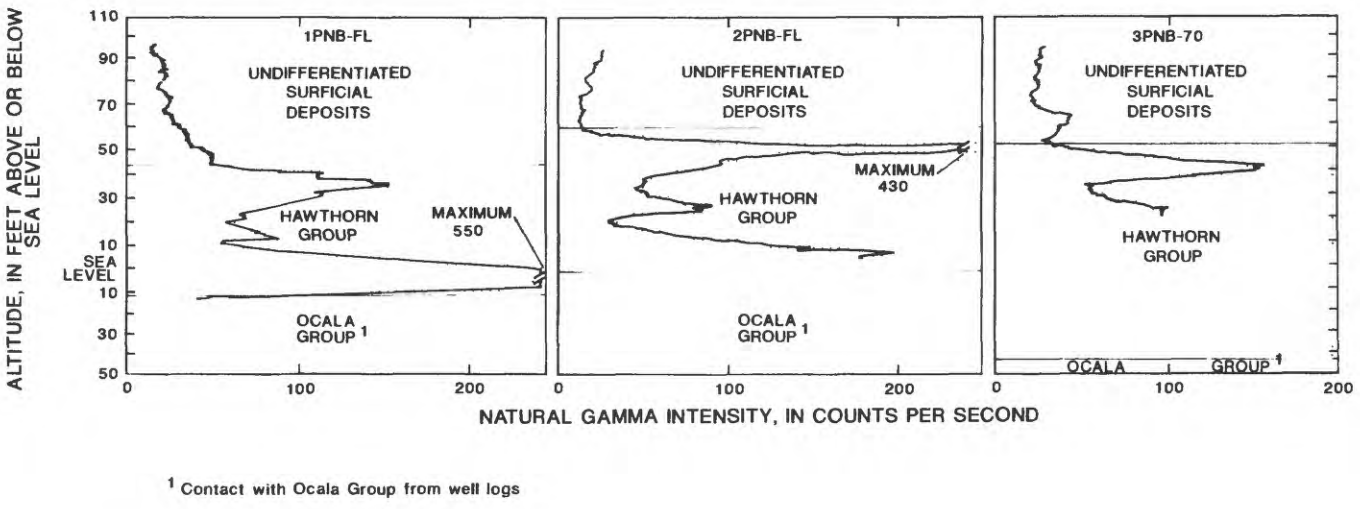

[1] Contact with Ocala Group from well logs

Figure 6. Natural-gamma radiation logs from the deepest well in each well nest.

Table 2. Description of observation wells in the basin surrounding Lake Barco

[All wells are 2 inches in diameter and screened except 1PNB-FL, which is 4 inches in diameter and has an open hole. Drilling method: A, auger; R, rotary; D, driven and jetted]

Well No.	Latitude–longitude		Well depth below land surface (feet)	Elevation of land surface (feet above sea level)	Length of screen or open interval (feet)	Drilling method
			Water-table wells			
WTB-1	294047	820030	44.7	139.0	5.0	A
WTB-2	294057	820028	49.9	156.1	5.0	A
WTB-4	294030	820019	39.8	115.9	5.0	A
WTB-5	294024	820020	29.3	98.9	5.0	A
WTB-6	294024	820032	33.5	99.4	5.0	A
WTB-6B	294026	820032	10.8	94.6	5.0	A
WTB-7	294023	820044	34.3	114.1	5.0	A
WTB-7B	294026	820041	29.5	108.9	5.0	A
WTB-9	294031	820044	29.2	109.0	2.5	A
WTB-10	294044	820039	54.5	133.9	5.0	A
WTB-12	294039	820024	11.8	95.5	5.0	A
WTB-13	294030	820023	8.4	92.3	5.0	A
WTB-14	294026	820024	21.9	95.9	5.0	A
WTB-15	294028	820038	14.1	96.3	5.0	A
WTB-17	294037	820037	14.1	97.5	5.0	A
WTB-18	294042	820034	13.7	97.4	5.0	A
WTB-19	294041	820030	9.5	92.5	5.0	A
WTB-20	294035	820024	22.9	97.3	4.0	A
WTB-21	294027	820033	13.9	91.4	4.0	A
WTB-22	294034	820039	11.3	92.6	4.0	A
			Nested wells			
1PNB-15	294042	820029	16.3	97.6	4.0	A
1PNB-20	294042	820029	21.3	98.0	2.5	A
1PNB-40	294042	820029	39.6	98.0	2.5	A
1PNB-60	294042	820029	63.2	98.0	2.5	A
1PNB-80	294042	820029	79.4	98.1	2.5	R
1PNB-FL	294042	820029	122	98.2	12	R
2PNB-18	294027	820025	18.8	93.3	4.0	A
2PNB-20	294027	820025	21.0	93.4	2.5	A
2PNB-40	294027	820025	40.4	93.3	2.5	A
2PNB-60	294027	820025	61.0	93.2	2.5	A
2PNB-80	294027	820025	81.7	93.3	2.5	A
2PNB-FL	294027	820025	102.9	93.5	5.0	R
3PNB-12	294031	820041	12.5	93.8	5.0	A
3PNB-20	294031	820041	21.4	94.3	2.5	A
3PNB-40	294031	820041	38.6	94.3	2.5	A
3PNB-50	294031	820041	50.2	94.4	2.5	A
3PNB-70	294031	820041	71.6	94.7	2.5	A
			Midlake wells[1]			
MLW-1	294039	820031	3.0	80.3	2.2	D
MLW-2	294039	820031	9.5	80.3	2.2	D
MLW-3	294035	820031	11.5	69.8	2.2	D
MLW-4	294033	820031	13.3	67.1	2.2	D
MLW-5	294030	820028	10.7	68.1	2.2	D
MLW-6	294028	820027	7.5	82.3	2.2	D

[1]Well depth is below lake bottom and elevation is of lake bottom for midlake wells.

The Hawthorn Group is not uniform in appearance at all well nests. At 1PNB, the upper Hawthorn Group has considerably more iron staining, as indicated by orange and red colors of the deposits. At 2PNB and 3PNB, the deposits are blue-gray, olive-gray, and tan. This difference may be related to oxygenated ground water on the north side of the lake and reducing conditions prevalent on the south or outflow side of the lake. A massive phosphatic sand bed approximately 7 ft thick is present immediately above the limestone at 2PNB. In contrast, the lower 10 ft of the Hawthorn Group at 1PNB consists of clayey sands with a decreasing coarse fraction. The Hawthorn Group ranges in thickness from about 60 ft at 1PNB and 2PNB to about 100 ft at 3PNB.

The contact with the limestone of the Ocala Group occurred at a similar altitude at 1PNB and 2PNB (12 and 3 ft below sea level, respectively). At 3PNB, however, where the well was drilled but not successfully completed in the limestone, the contact with the limestone was approximately 40 ft deeper at an altitude of 46 ft below sea level. Because of the highly weathered, karst nature of the limestone surface, irregularities such as this are not unusual in the study area (Bermes and others, 1963; Scott, 1983).

Evidence of Karst Features in the Basin

Several ground-penetrating radar (GPR) transects were made in the basin around Lake Barco. GPR has been successfully used in other parts of Florida to map subsidence features associated with karst activity (Beck and Wilson, 1988; J.T. Trommer, U.S. Geological Survey, written commun., 1990). The return radar signal is a function of the electromagnetic properties of the media it is traveling through. Heterogeneities in the media, such as changes in moisture content at the water table or increased clay content, are seen as reflective surfaces. These surfaces can then be mapped in transects. Signal attenuation also is a function of the media, and clay-rich strata will attenuate the signal much faster than sandy strata.

Results from GPR transects in the basin illustrate downwarping of beds within the surficial deposits, particularly near the lake. Reflective surfaces, most likely beds of increased clay content, were mapped on several transects (fig. 7). The hummocky irregularity and downward-dipping nature of these reflective surfaces suggest that subsidence of deeper structural features has occurred at some time in the past. In some instances, dipping beds are overlain by more horizontal beds, which may be infilled sands (for example near well WTB-18, fig. 7). The lack of surficial expression of these dipping beds also indicates significant amounts of infilling.

The GPR signal generally did not penetrate deeply enough to map the top of the Hawthorn Group. It is reasonable to assume that the contact with the Hawthorn Group

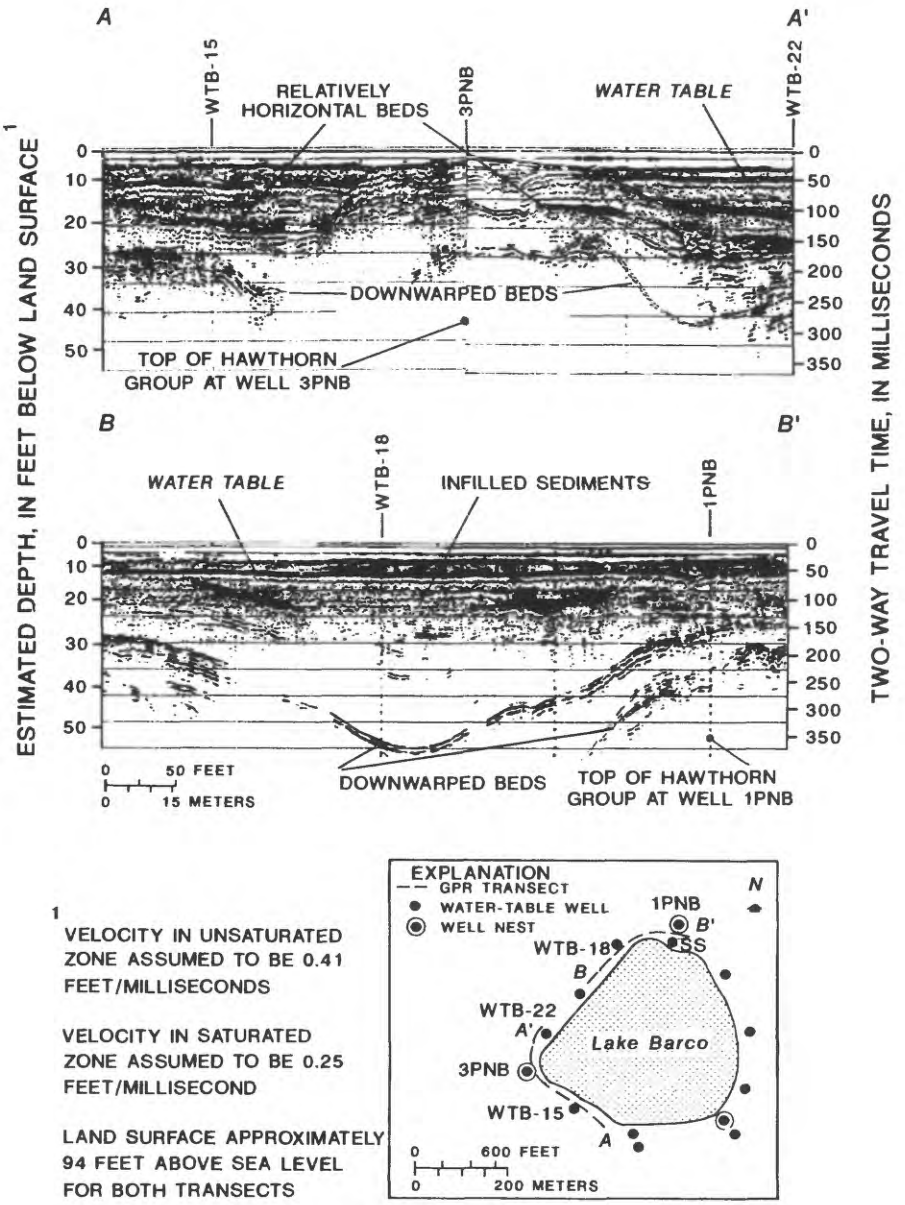

Figure 7. Ground-penetrating radar record illustrating subsidence features near Lake Barco.

occurs deeper where downwarping beds occur in the surficial deposits. Thus, the lithology is not laterally homogeneous and may not be continuous, particularly below the lake. Local variability in the stratigraphy also was noted at the site where the split-spoon sample was collected (fig. 5, site SS), about 75 ft south of 1PNB toward the lake. The hole was drilled to 66 ft (or 26 ft above sea level), which is almost 20 ft below the contact with the Hawthorn Formation at 1PNB. Deposits at this site were generally uniform, light-colored sands, and no indication of the Hawthorn Group, as seen at 1PNB, was observed. This suggests that the deposits may be infill material associated with lake-structure subsidence and that the Hawthorn Group occurs at a considerably greater depth at this site.

At 3PNB where the top of the limestone is 40 ft deeper than at 1PNB, the surficial deposits appear to be laterally continuous. The GPR record illustrates a relatively horizontal trend in the beds at this site (fig. 7). This trend also is evidenced in the stratigraphy because the top of the Hawthorn Group is at a similar altitude at all three well nests. Thus, the irregularity in the limestone surface at 3PNB probably is not the result of recent karst activity, but, rather, may have occurred at a time before the entire Hawthorn Group was deposited.

To summarize, downward-dipping beds occurring in the surficial deposits illustrate karst activity within the basin. These depressions are not noted at land surface because of infilling with sands. The downwarping of beds within the surficial deposits suggests that the intermediate confining unit within the Hawthorn Group is not at the same altitude in the basin and could be breached in places. Older karst activity also has occurred, as illustrated by relatively lateral beds occurring in the surficial deposits at a location where the limestone is found at significantly greater depth.

Sublake Geology

A map of the thickness of the soft, organic-rich lake sediments was created from probe-rod measurements (fig. 8). These sediments, which are generally black to very dark green with very little sand content, are focused primarily in the deepest part of the lake. More than 10 ft of sediments occur in these areas. The southern half of the lake has considerably less sediments than the northern half of the lake because of the steeper slope of the northern lakebed. When sediment thickness is plotted in cross section with the lake bathymetry, the lake basin is more rounded than the relatively flat lake bathymetry (fig. 8).

Additional sediment thickness measurements were made when six "midlake" wells were driven and jetted into the surficial deposits beneath the lake sediments. These wells were installed along a transect through the lake (fig. 5, denoted as MLW) to provide data on head distribution below the lake. Construction information on these wells is included in table 2. Observed sediment thickness compared well with previous probe-rod measurements. Samples from the sublake surficial deposits below the organic-rich sediments range from clean sands to relatively hard clay.

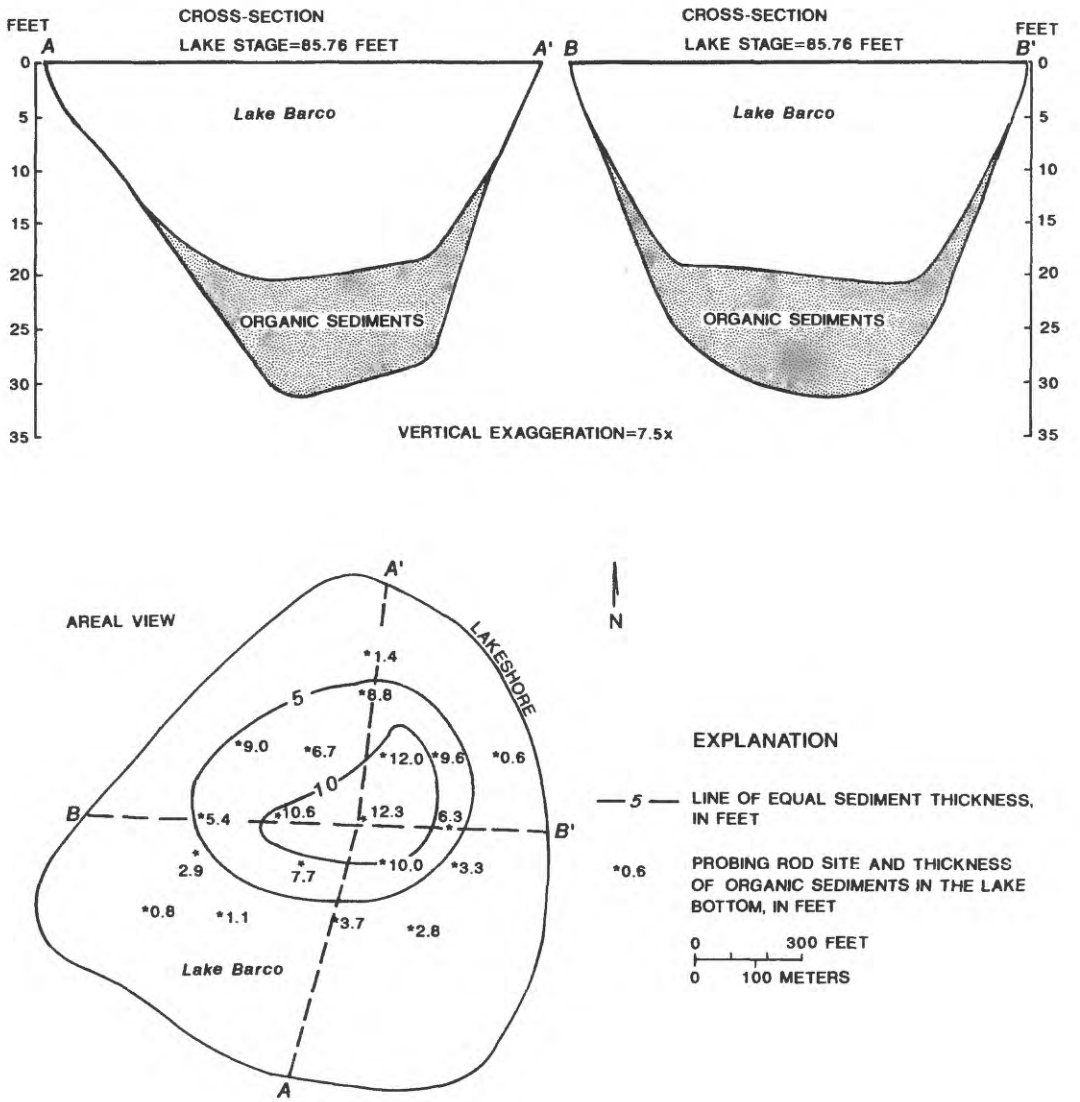

Figure 8. Thickness of organic-rich sediments beneath Lake Barco.

A GPR survey was conducted over the lake surface to gain additional information about sublake geology. The GPR record confirmed sediment thickness measurements, but the radar signal was able to penetrate only a short distance below the lake sediments. Multiples of the sediment-water interface interfered with the reflected signal near the shoreline where sediment thickness is minimal. Reflectors at a steeper angle than the multiples occurred immediately offshore. This may indicate steeply dipping beds or a bed that was breached at the near-shore margins of the lake. Confirmation of the nature of this reflector, however, could not be made.

A seismic-reflection survey also was conducted on Lake Barco to examine deeper geologic structures below the lake. Other lake studies have incorporated similar seismic-reflection data to enhance the knowledge and understanding of sublake geologic structures (Locker and others, 1988; Snyder and others, 1989; Lee and others, 1991). The survey employed an ORE-geopulse continuous profiling system with a sound source operating at 175 J. The received signal was filtered from 600 to 2,000 Hz. The sound source was towed alongside a boat, and the hydrophones were towed approximately 20 ft off the stern. Navigation was provided by visual reckoning on 13 marked points spaced evenly around the shoreline of the lake. Survey transects included a perimeter run and numerous cross-lake patterns. Areas of the lake where thick organic sediments occur were avoided because the gas associated with them impeded the seismic signal and did not render interpretable record. The most useful transects were focused around the perimeter and the southern part of the lake where organic-rich sediments were thin or nonexistent.

Lithologic data from the three well nests, 1PNB, 2PNB, and 3PNB, were used for geologic control in the seismic-data interpretation. Depths to limestone were projected to the edge of the lake from the three control wells. These depths were converted to milliseconds and compared to the seismic record. A velocity value of 1,800 m/s was used for converting from traveltimes to depths. This value represents an average velocity of unconsolidated surficial sediments similar to those found in the study area (McQuillan and Ardus, 1977; Sheriff, 1980; A.L. Hine, University of South Florida, written commun., 1986).

The reflector, assumed to be the limestone surface, was well defined in limited parts of the record. In these sections, the signal generated by the limestone surface was unique compared to overlying reflectors and was easily discerned. An example of the reflector assumed to be the limestone surface is presented in figure 9. In most of the transects, however, there were small windows of interpretable data surrounded by record that was seismically clear, chaotic, or contained abundant multiples and "ringing." Parts of the seismic record where the limestone surface could not be identified were analyzed for trends. These trends were extrapolated from nearby interpretable data and from lithologic control points and were incorporated into the structural contour map as inferred data. Cross-lake transects where sediments were thin or absent were generally interpretable, whereas transects crossing the thick lake sediments resulted in little interpretable data. Reflectors above the limestone surface were observed in some of the record, but they were often obscured by multiples and were difficult to follow continuously. These shallower reflectors were not mapped due to the discontinuous nature of the signal and the uncertainty associated with identifying them.

The resulting structural contour map shows the variability in the depth to the limestone surface below the lake (fig. 10). One of the prominent features in this surface is a depression below the southwestern part of the lake. This depression appears to be a subsidence feature based on trends in several crossing transects, although the limestone reflector was not observed. Geologic data at 3PNB indicate that this depression extends at least 40 ft below the limestone surface seen in 1PNB and 2PNB. Another depressional structure was observed offshore from 2PNB. This structure is coincident with a depression in the topography that extends onshore toward the southeast (fig. 4). There is a structural high in the limestone surface on the southern side of the lake between these two depressional features. Although no interpretable record is available for the center of the lake, the limestone surface observed below the lake margin dips toward the center, which indicates that additional subsidence features may be located in this area (fig. 11). In addition, the thick accumulation of lake sediments and the slope of the lakebed in the center of the lake indicates that the structure responsible for the formation of the lake occurs within this area.

The geologic information gathered during this study indicates that Lake Barco is underlain by an irregular limestone surface and is the result of sinkhole subsidence activity. Whether the lake is the result of one major subsidence structure or the composite of many smaller sinkhole features cannot be determined. Data obtained from the southern part of the lake provide an indication of the possible complexity involved in the sublake geology. Due to the incomplete coverage of interpretable sublake data, the exact distribution of the karst features below the lake is unknown.

The presence of subsidence features and a karstified limestone surface indicates that the Hawthorn Formation and surficial deposits below the lake do not consist of coherent, continuous beds. Rather, beds are disrupted because of subsidence activity and the associated infilling of solution voids in the limestone (fig. 11). Many lakes of sinkhole origin have been formed when surficial sand and clay deposits were "piped" into solution features in the underlying limestone (Sinclair and Stewart, 1985; Lane, 1986; Lee and others, 1991). This piping creates disruptions in the overlying layers that result in slumping and subsidence in sandy beds and ruptures or breaks in clay beds. Such collapse features in the sublake geology and associated infilling of surficial sediments may increase the potential for hydraulic connection between the lake and Upper Floridan aquifer (Lee and others, 1991).

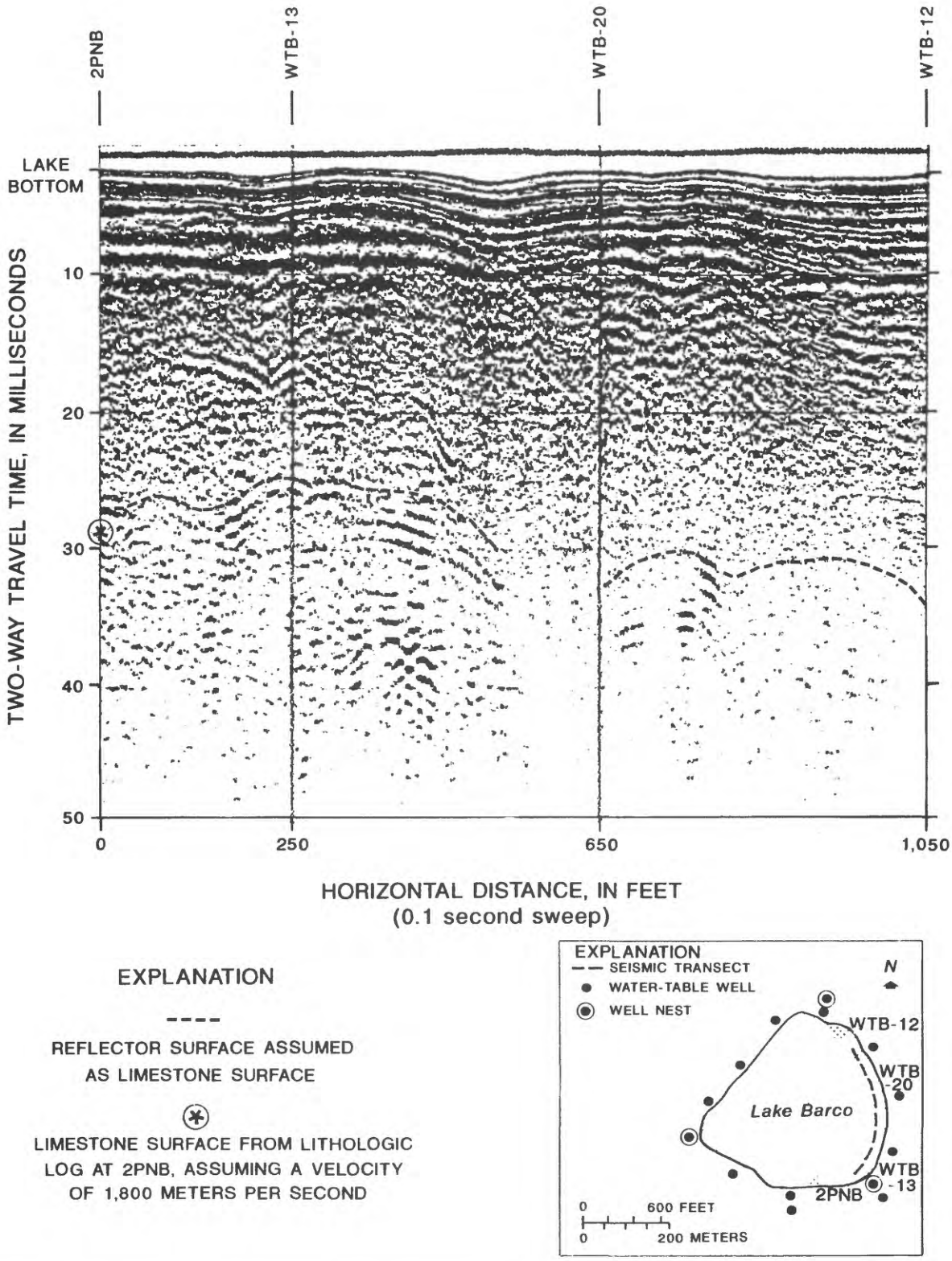

Figure 9. Seismic-reflection record showing reflector surface interpreted as the limestone surface.

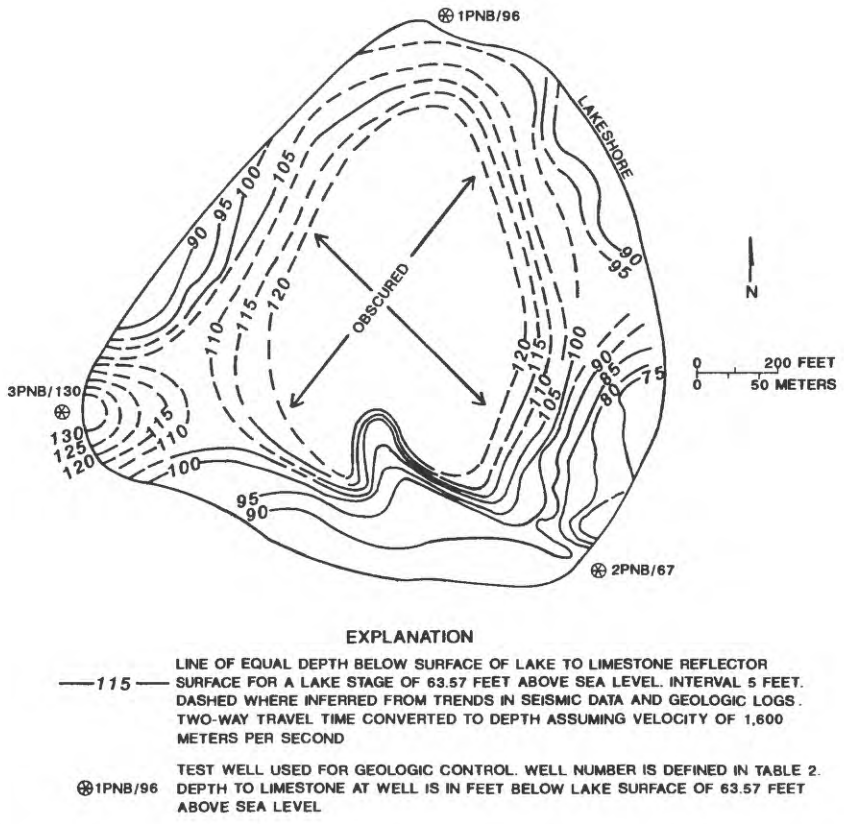

Figure 10. Structural contours of the limestone surface below Lake Barco as indicated from seismic-reflection record.

The thickness of the sediments and estimates of recent sediment deposition rates indicates that the lake is at least 1,000 years old. Given recent deposition rates from Pb-210 dating (R.W. Bienert, Jr., University of Florida, written commun., 1989) of 11 cm per 130 years, or approximately 1 mm/yr, it would take more than 3,600 years to deposit 12 ft of sediment in the lake. Differences between historical and recent deposition rates may increase or decrease this estimate.

METHODS AND INSTRUMENTATION TO COMPUTE THE HYDROLOGIC BUDGET

The basic hydrologic-budget equation of a lake states that change in lake volume for a given time period is equal to the sum of the water inflows and outflows and the errors in measurement over the same time period. Surface-water inflow and outflow are not present in the hydrologic budget of a seepage lake, and the contribution from overland flow is considered to be negligible in the study area due to the extremely permeable surficial materials in the basin. The influence of measurement errors of each of these hydrologic-budget components is extremely important to the interpretation of the final hydrologic budget (Winter, 1981). Representing these errors results in the following form of the hydrologic-budget equation:

$$\Delta S \pm e_S = P \pm e_P - E \pm e_E + GI \pm e_{GI} - GO \pm e_{GO} \qquad (1)$$

where

ΔS is change in lake storage for a discrete time period, in inches;
P is precipitation, in inches;
E is total evaporation, in inches;
GI is total ground-water inflow, in inches;
GO is total lake leakage, in inches; and
e is the error in measurement of each budget component, in inches.

Volume is represented in units of length by dividing by lake surface area. At Lake Barco, the hydrologic monitoring network included measurements of lake stage, precipitation, climatological variables necessary to compute evaporation, and ground-water gradients to compute the ground-water flux. The following sections describe the methods and instrumentation used to estimate individual components of the hydrologic budget of the lake.

Evaporation

Because lake evaporation cannot be measured directly, approaches to estimating evaporation generally rely upon measuring related climatic variables and calculating evaporation. The energy-budget method is considered to be one of the most accurate methods for calculating evaporation

(Winter, 1981) and is the primary method being employed at Lake Barco. The water lost by evaporation is determined from the difference between the change in energy stored by the lake and the net gain or loss of energy to the lake for the same time period. This difference represents the energy required as latent heat of vaporization to evaporate a volume of water from the lake.

To define the energy balance of the lake, climatic variables must be measured. Methods being used in this study closely parallel those used in the study of the hydrologic budget of Lake Lucerne in Florida (Lee and others, 1991; T.M. Lee and Amy Swancar, U.S. Geological Survey, written commun., 1990). A thorough discussion of the instrumentation used in energy-budget and mass-transfer evaporation studies is given by Sturrock (1985). The energy-balance equation can be expressed as:

$$Q_s - Q_r + Q_a - Q_{ar} - Q_{bs} + Q_v - Q_w - Q_h - Q_e = Q_x \qquad (2)$$

where

Q_s is incoming shortwave radiation,
Q_r is reflected shortwave radiation,
Q_a is incoming longwave radiation,
Q_{ar} is reflected longwave radiation,
Q_{bs} is backscattered longwave radiation emitted from the lake,
Q_v is energy advected into the lake,
Q_w is energy advected by evaporating water,
Q_h is energy conducted from the lake by the atmosphere as sensible heat,
Q_e is energy used for evaporation, and
Q_x is change in stored energy.

The units of energy for each term are calories per square centimeter per day. The above equation assumes that conduction of heat through the lake bottom, heating due to chemical and biological processes, and the conversion of kinetic energy to heat energy are negligible. Development of the theory behind the energy-budget method is discussed in detail by Anderson (1954) and Ficke (1972).

Evaporation also will be estimated from a second approach, the mass-transfer method. This method is less accurate, but is considerably simpler than the energy-budget method. In addition, most of the required climatic data were collected for the energy-budget method. This method relies on the calibration of the empirical mass-transfer coefficient with an independent estimation of evaporation. Evaporation computed from the energy-budget method will be used

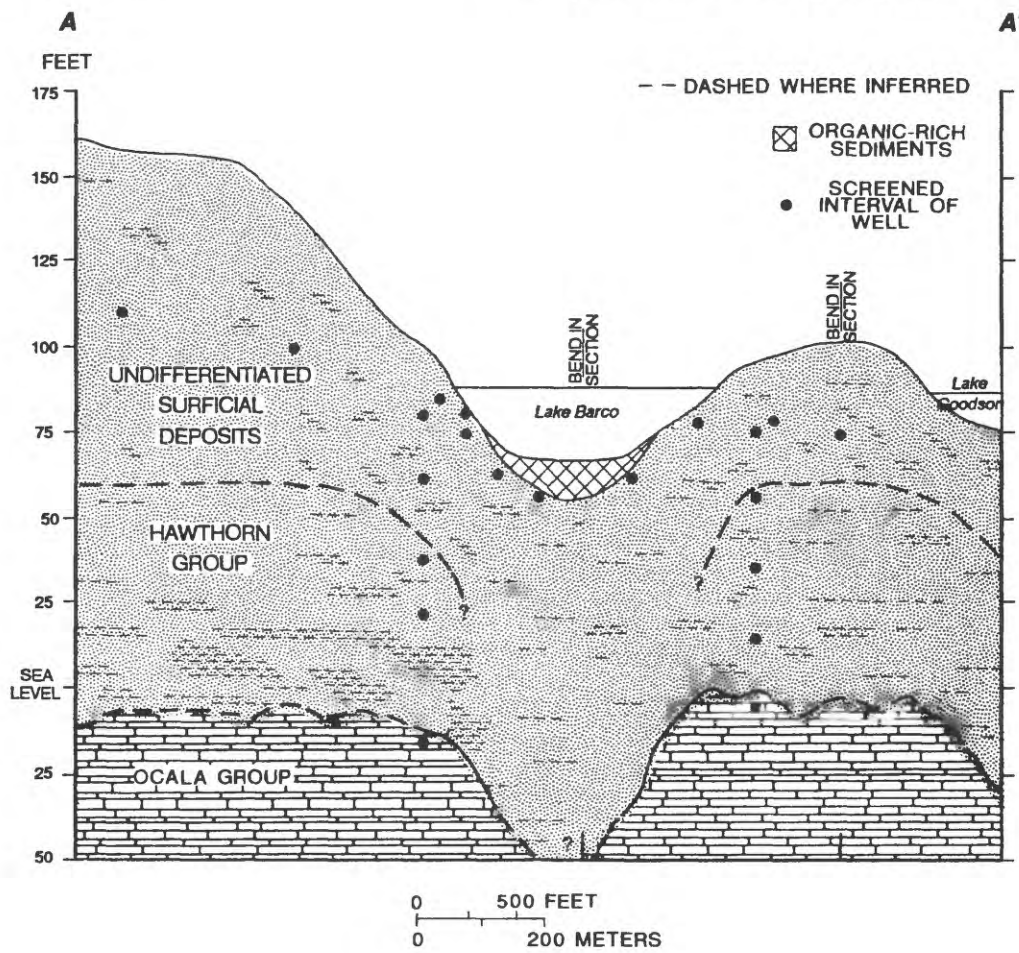

Figure 11. Geologic section through Lake Barco showing features delineated by seismic and lithologic data. (Location of section is shown in fig. 5.)

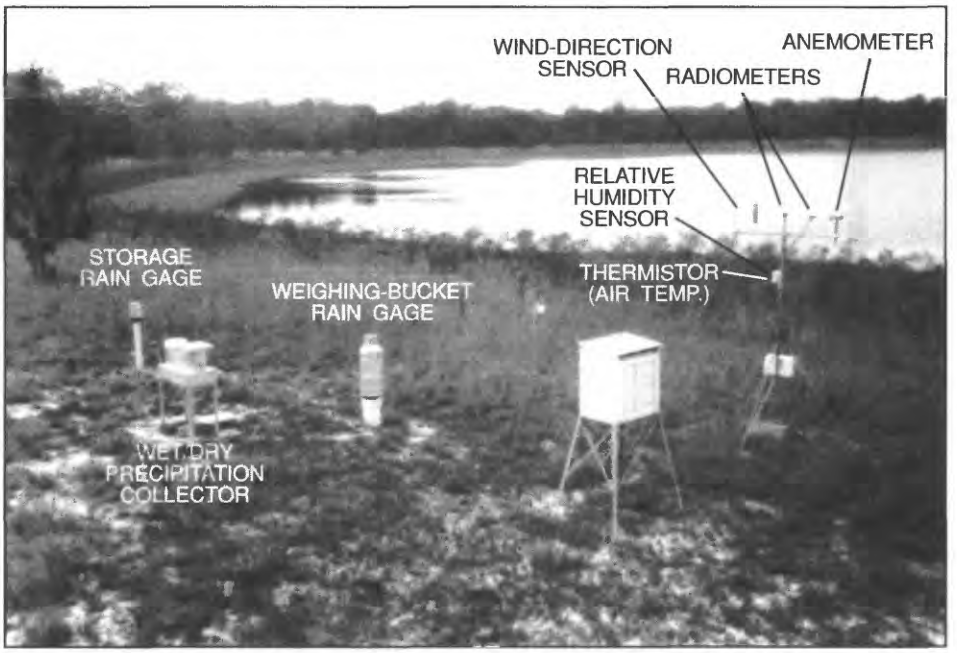

Figure 12. Instrumentation at land-based climate station.

to calibrate this coefficient. Evaporation estimates from the mass-transfer method can then be compared with the energy-budget evaporation estimates to determine whether the mass-transfer approach can be used to estimate evaporation accurately in future studies using considerably less instrumentation.

The mass-transfer approach assumes that evaporation rates are controlled by windspeed and vapor-pressure gradients between the lake surface and the air (Anderson and others, 1950). The mass-transfer equation of Harbeck (1962), used in this study, is:

$$E_{MT} = N\, u_2\, (e_o - e_a) \qquad (3)$$

where

E_{MT} is evaporation from the lake surface, in centimeters per day;
N is an empirical mass-transfer coefficient, in centimeters per day per miles per hour times millibars;
u_2 is windspeed at 2 m above the water surface, in miles per hour;
e_o is saturation vapor pressure of the air at the temperature of the water surface, in millibars; and
e_a is vapor pressure of the air 2 m above the water surface, in millibars.

Climatic data at Lake Barco were collected at a land-based climate station and at a raft-based climate station. At each climate station, a data logger was used to read and store the electronic signal received every 60 s from individual climate sensors. These sensor inputs were processed and output by the data logger to a storage module as the hourly and daily means or totals of the climatic variable. The land-based climate station was on the north side of the lake, approximately 75 ft from the lakeshore. Variables monitored at the land-climate station included air temperature, windspeed and direction, relative humidity, incoming longwave and shortwave radiation, and precipitation (fig. 12, table 3).

The raft-based climate station was a floating platform anchored in the deepest part of the lake. Variables continuously measured at the raft-based climate station at 2 m (6.6 ft) above the water surface were air temperature, windspeed, wet-bulb and dry-bulb temperatures, and relative humidity. Water-surface temperature and the temperature profile of the lake at 1-ft intervals also were measured from the raft (fig. 13, table 3). Temperature profiles are required to compute the stored heat in the lake. In addition, thermal surveys, or vertical water-temperature measurements at 1-ft intervals from five stations in the lake, were made on a weekly basis.

Precipitation

Rainfall was measured at three rain gages at the Lake Barco land-based climate station (fig. 12). Rainfall was monitored continuously with a tipping-bucket rain gage. The data were electronically recorded and processed by a data logger and output as hourly and daily totals. Rainfall also was measured in a weighing-bucket rain gage that records the data on an analog chart recorder. Cumulative weekly rainfall volume was measured using a storage rain gage.

Table 3. Instrumentation used at the Lake Barco climate stations

[mi/h, mile per hour; °C, degree Celsius; (cal/cm^2)/d, calorie per square centimeter per day; in/d, inch per day; in., inch]

Instrument type	Supplier[1]	Model	Purpose/measurement/units
Land-based climate station			
Data storage/retrieval equipment and sensor mounts			
Data logger	Campbell	CR10	Store continuous data
64K option in CR10	Campbell		Additional data storage
Enclosure for CR10	Campbell	021/LA	Enclosure for CR10
Key pad/display/CR10	Campbell	CR10KD	Key pad for interfacing CR10
Storage module	Campbell	SM192	External data storage
Tripod with grounding kit	Campbell	CM10	Support for sensors
Cross arm sensor mount	Campbell	019	Support for sensors
Solar panel with mounts	Campbell	SX10	Recharge battery
Weather shelter	Qualmetrics	NWS specs	Enclosure for backup instruments
Climatic sensors			
Anemometer	MetOne	014A	Windspeed (mi/h)
Wind-direction sensor	Campbell	024A	Wind direction (0-360 degrees clockwise from north)
Temperature and relative humidity	Campbell	207	Temperature (°C) and percent relative and humidity
12-plate Gill radiation shield for RH sensor	Campbell	41004-5	Shield sensor
Radiometer	Eppley	PSP	Incoming shortwave radiation [(cal/cm^2)/d]
Radiometer	Eppley	PIR	Incoming longwave radiation [(cal/cm^2)/d]
Tipping-bucket rain gage	Campbell	TE525	Rainfall intensity and volume (in/d)
Assman psychrometer	Qualmetrics	5230	Wet- and dry-bulb temperature (°C)
Weighing-bucket rain gage	Belfort	5-780	Record cumulative rainfall (in.)
Wet/dry precipitation collector	Aerochem Metrics	301	Collect wet and dry atmospheric deposition
Storage rain gage	Qualimetrics	6340	Record cumulative rainfall (in.)
Raft-based climate station			
Data storage/retrieval equipment and sensor mounts			
Data logger	Campbell	CR10	Store continuous data
64K option in CR10	Campbell	EM10-64	Additional data storage
Enclosure for CR10	Campbell	021/LA	Enclosure for CR10
Multiplexer	Campbell	AM32	Additional signal input to CR10
Solar panel	Campbell	SX10	Recharge battery
Reference temperature for CR10	Campbell	10TCRT	Internal reference temperature for CR10
Spark-gap junction box	Campbell	036	J-box with spark gaps
Raft	USGS		Platform to mount sensors
Climatic sensors			
Thermocouple cable	Campbell	105T	Vertical profile water temperature (°C)
Water-surface temperature probe	Campbell		Water-surface temperature (°C)
Nonventilated thermocouple	USGS	HIF	Wet- and dry-bulb temperature (°C)
Temperature and relative humidity	Campbell	207	Temperature (°C) and percent relative humidity
Anemometer	MetOne	014A	Windspeed (mi/h)
12-plate Gill radiation shield for RH sensor	Campbell	41004-5	Shield sensor

[1]Use of brand names is for descriptive purposes only and does not constitute endorsement by the U.S. Geological Survey.

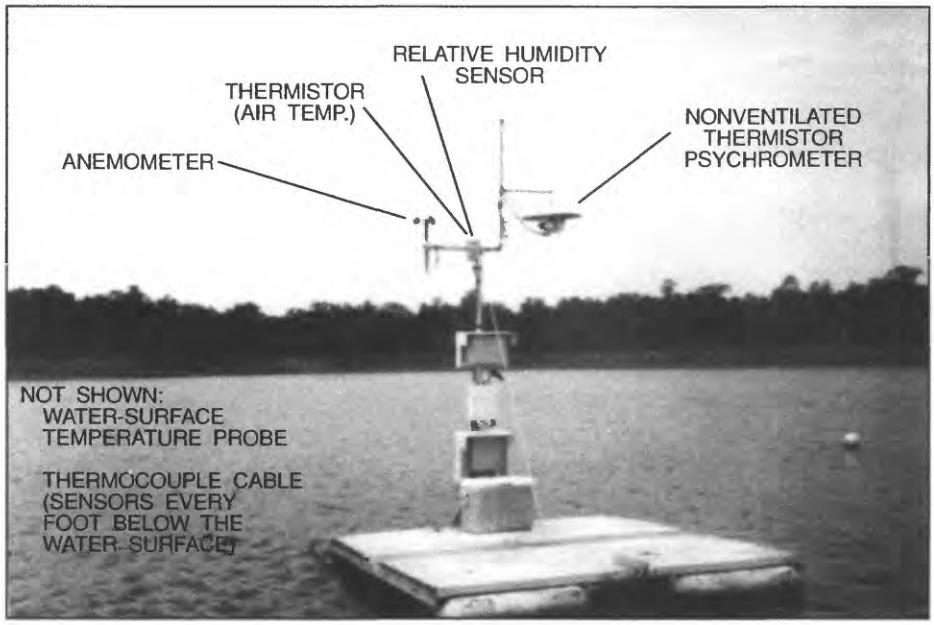

Figure 13. Instrumentation at raft-based climate station.

Lake Storage

Hourly and daily stage values were measured by a recording stage gage between March 8, 1989, and April 13, 1990. After this, the stage was read weekly from a staff gage. To calculate lake storage from lake stage, a bathymetric survey of the lake was conducted. From the information on lake-bottom morphology, stage-volume and stage-area relations were determined.

Ground Water

Ground-water inflow to the lake and lake leakage to the surficial aquifer system are difficult terms to quantify because direct measurements are not feasible. The interaction of ground water with the lake is determined largely by the local hydrogeology. Ground-water fluxes can be computed as a function of the hydraulic properties of the geologic materials surrounding the lake, namely hydraulic conductivity and specific yield. In addition, information is needed on the vertical and horizontal distribution of hydraulic head in the ground-water system and any external sources or sinks of water to the system (such as ground-water pumping). These data can be used to solve some formulation of the transient ground-water flow equation in three dimensions:

$$\frac{\partial}{\partial x}\left(K_{xx}\frac{\partial h}{\partial x}\right)+\frac{\partial}{\partial y}\left(K_{yy}\frac{\partial h}{\partial y}\right)+\frac{\partial}{\partial z}\left(K_{zz}\frac{\partial h}{\partial z}\right)-W=S_s\frac{\partial h}{\partial t} \quad (4)$$

where

K_{xx}, K_{yy}, and K_{zz} are values of hydraulic conductivity along the x, y, and z coordinate axes, which are assumed to be parallel to the major axes of hydraulic conductivity, in feet per day;

h is the hydraulic head, in feet;

W is a volumetric flux per unit volume and represents sources and sinks of water, in day^{-1};

S_s is the specific storage of the porous material, in $feet^{-1}$; and

t is time, in days.

This equation, or adaptations of this equation, can be solved numerically using finite-difference approximations (Winter, 1976; McDonald and Harbaugh, 1988). Further simplifying assumptions, for example, of steady-state conditions of one- or two-dimensional flow can be used to solve this equation analytically or graphically by flow-net analysis (Bear, 1979).

Hydraulic head in the aquifers surrounding Lake Barco was monitored using the network of observation wells drilled in the basin (fig. 5, table 2). This network includes 20 wells finished in the upper part of the surficial aquifer system for monitoring the altitude of the water table around the lake and three groups of nested wells finished at various depths between the water table and the underlying Upper Floridan aquifer. In addition to wells in the surrounding basin, the head below the lake sediments was monitored in the six midlake wells. The vertical distribution of wells in the vicinity of Lake Barco is illustrated in figure 14. Water levels in the wells were measured on a biweekly basis. Later in the study, weekly water-level measurements were made in

selected wells close to the lake. To better define the lateral boundaries of the ground-water system, staff gages were installed on surrounding Lake Goodson, Lake Rowan, and Long Lake. The stages of these lakes generally were read weekly for approximately 1 year.

PRELIMINARY ANALYSIS OF DATA TO COMPUTE THE HYDROLOGIC BUDGET

Data are presented that will be used to compute the hydrologic budget of Lake Barco. This summary includes climatological data necessary to compute evaporation, the amount of precipitation during the study period, the change in lake stage and volume, and the hydraulic head distribution in the aquifers near the lake. The actual hydrologic budget is planned for presentation in a future report.

Evaporation

Climatological variables measured at the land-based climate and raft-based climate stations generally varied in response to two distinct seasonal periods: the warmer, wetter summer months between May and September and the cooler, drier months from October to April (fig. 15). The range of these variables over the period of record is summarized in table 4. Daily total longwave radiation was fairly constant between May and September, but was highly variable between October and April (fig. 15a). This seasonal variability is due to the temperature and moisture content of the air. Daily total incoming shortwave radiation varies sinusoidally during the year (fig. 15b), with highest values occurring near the summer solstice (June 21) and lowest values occurring near the winter solstice (December 21). Scatter along this sinusoidal curve is related to cloud cover. Monthly total longwave and shortwave radiation are shown in figure 16.

Climatological data from the land-based climate station were not available for a 20-day period between November 6 and November 26, 1989, when an internal battery on a storage module failed. A regression equation with vapor pressure was used to estimate missing values of longwave radiation (table 5). Missing shortwave radiation for this period was estimated from data collected at a research site near Gainesville (J.W. Mishoe, University of Florida, written commun., 1990). Photosynthetically active radiation (PAR), which includes light in the waveband wavelengths between 400 and 700 nm, had the best correlation with shortwave radiation at the Lake Barco site. This regression equation was used to estimate shortwave radiation when PAR data were available (table 5). When PAR data were not available, a regression equation with total radiation at the Gainesville site was used to estimate shortwave radiation (table 5).

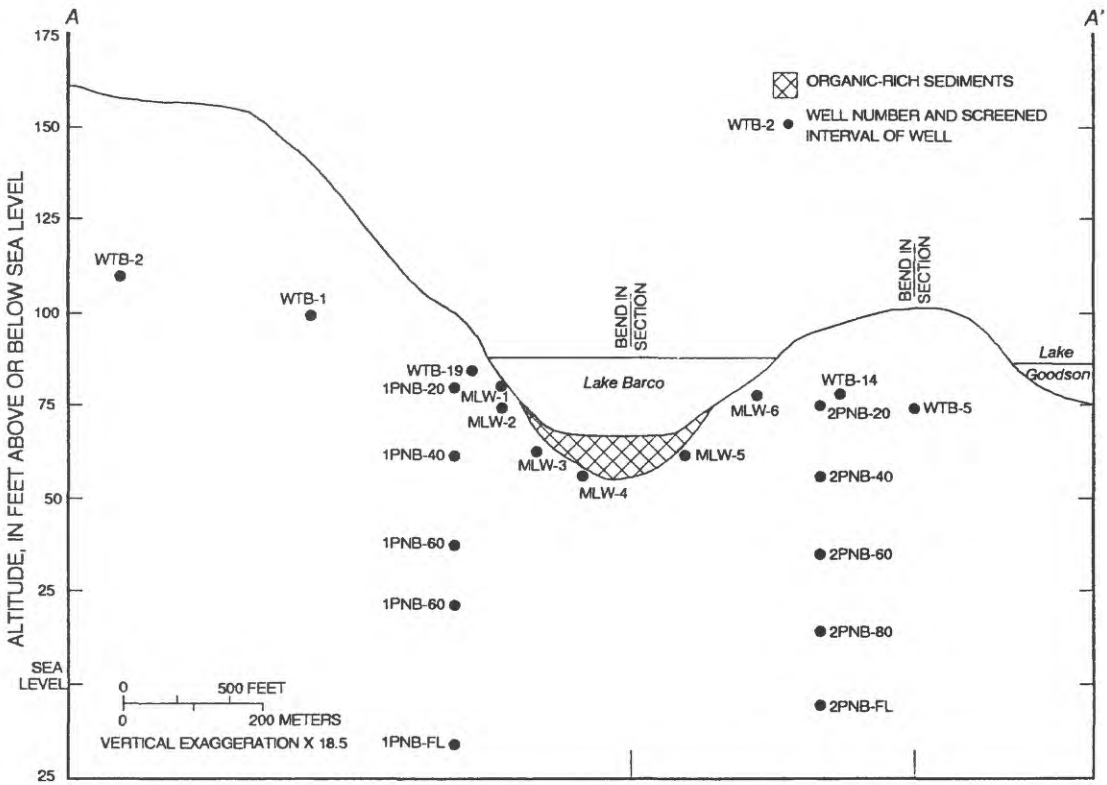

Figure 14. Cross section through Lake Barco showing vertical distribution of well network. (Location of section is shown in fig. 5.)

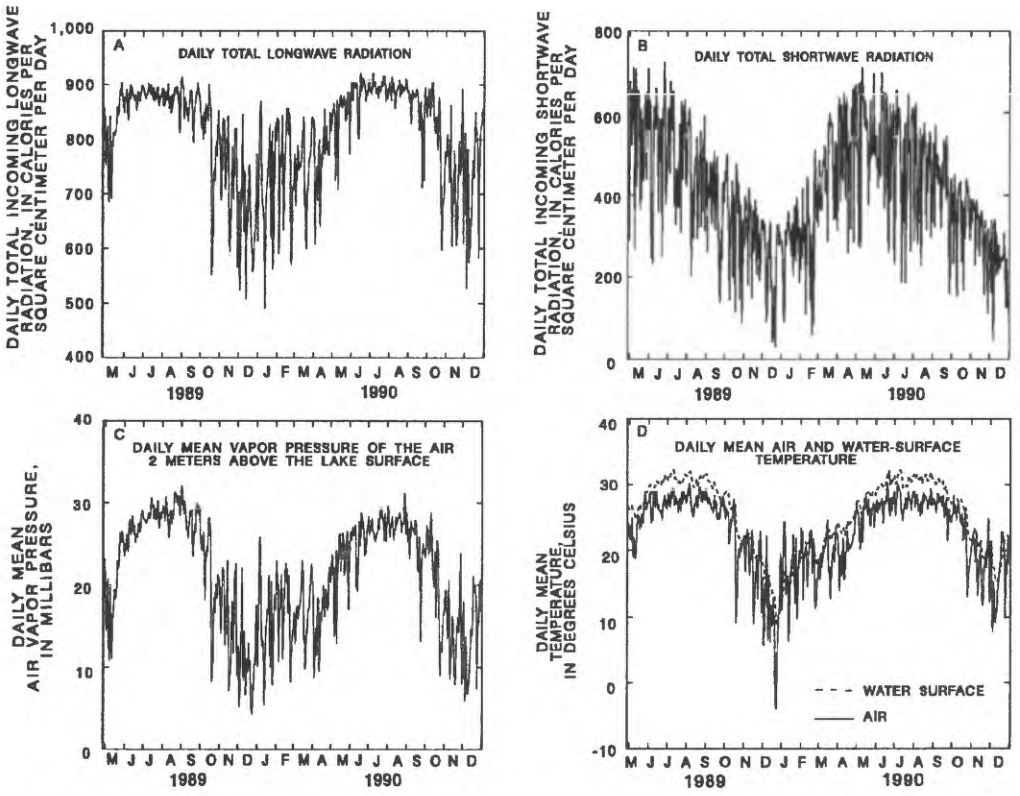

Figure 15. Variability of daily total incoming longwave radiation (A), daily total incoming shortwave radiation (B), daily mean air-vapor pressure of the air (C), and daily mean air and water-surface temperature (D) during the period of record.

The moisture content of the air is presented as vapor pressure. The most accurate method of calculating vapor pressure is from wet- and dry-bulb temperatures. The nonventilated thermocouple psychrometer, however, was not working properly during most of the first year of data collection. Thus, vapor pressure was calculated for much of the period of record from relative humidity and air temperature measured at the raft. According to onsite inspections with a ventilated psychrometer, readings from the relative humidity sensor at the raft were slowly declining with time (fig. 17). A time-dependent regression equation (table 5) was used to correct vapor pressure until April 1990. Between April and June 1990, vapor pressure was estimated from a regression equation using vapor pressure calculated from the relative humidity sensor (table 5). Vapor pressure calculated from this regression compared more favorably to vapor pressure from the nonventilated psychrometer during periods of overlapping record between May and July 1990. The time dependent relation slightly overestimated vapor pressure during this period. The relative humidity sensor on the raft was replaced in July 1990, so a different regression equation with vapor pressure calculated from the relative humidity sensor was used when the nonventilated psychrometer malfunctioned during a period in September and October

Table 4. Summary statistics for climatic data

[mb, millibars; °C, degree Celsius; mi/h, mile per hour; (cal/cm^2)/d, calorie per square centimeter per day; ft, feet]

Variable	Daily mean or total	Mean	Median	Minimum	Maximum	Standard deviation
Vapor pressure (mb)	Mean	21.1	22.4	4.4	32.0	6.7
Air temperature (°C)	Mean	22.5	24.6	-4.0	30.0	5.8
Windspeed (mi/h)	Mean	4.2	4.0	1.8	9.3	1.1
Longwave radiation [(cal/cm2)/d]	Total	809	840	491	921	91
Shortwave radiation [(cal/cm2)/d]	Total	408	403	29	723	149
Water surface temperature (°C)	Mean	25.6	27.5	8.9	32.8	5.7
Water temperature 5 ft (°C)	Mean	25.4	27.3	8.9	32.7	5.7
Water temperature 10 ft (°C)	Mean	25.1	27.1	8.7	32.5	5.7
Water temperature 15 ft (°C)	Mean	25.0	27.0	8.8	32.5	5.7

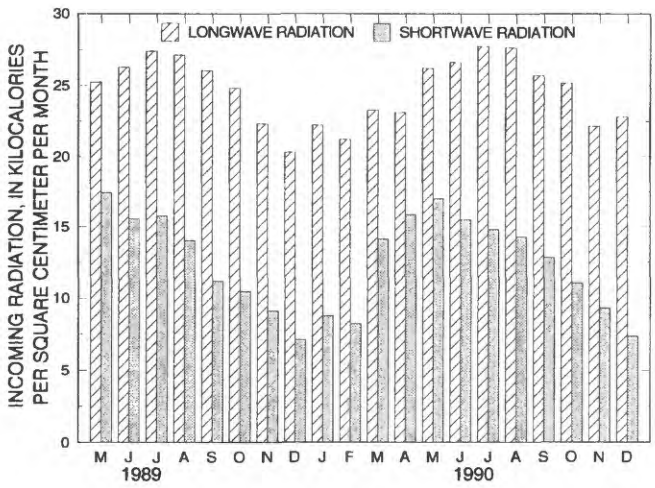

Figure 16. Monthly total incoming longwave and shortwave radiation.

1990 (table 5). Daily mean vapor pressure of the air was high during the summer months and relatively constant at about 30 mb (fig. 15c). During other times of the year, vapor pressure was considerably lower and more variable, ranging from 5 to 25 mb.

Daily mean water-surface and air temperatures followed parallel patterns, but lake temperature was more moderated and often lagged compared to air temperature (fig. 15d). Daily mean water-surface temperature was generally warmer than daily mean air temperature, particularly between March and October. Daily mean water-surface temperature ranged from a high of 32.8°C in July 1989 to a low of 8.9°C in December 1989; daily mean air temperature ranged from a high of 30.0°C to a low of -4.0°C. The lake does not thermally stratify, and there was generally less than 1°C difference between daily mean temperatures at the surface and at the 15-ft depth. A regression equation with the temperature from the top thermocouple sensor was used to estimate water-surface temperature for several periods when water-surface temperature data were missing (table 5).

Average water-temperature profiles, computed as the mean of the vertical temperature profiles from the five thermal survey stations, compared closely with the daily mean temperature profiles measured at the raft by the thermocouple string. Representative regression equations are presented for the 5- and 10-ft depths in table 5. Daily measurements provided by the thermocouple string at the raft appear to be a good indicator of the spatially averaged lake temperature derived from thermal-survey measurements. Therefore, heat storage in the lake and, in turn, evaporation can be calculated on a daily basis as well as by thermal-survey period.

Precipitation

The storage rain gage, which was added to the site in late September 1989, provided the most reliable measurement of rainfall during the period of record. The tipping-bucket rain gage had low readings during high-intensity storms. Because the error in the rainfall measured by the tipping bucket is a function of rainfall intensity, the data were adjusted according to the daily rainfall volume. Comparisons were made between weekly rainfall from the storage rain gage and daily rainfall from the tipping bucket totaled by week. The best agreement between the two gages occurred when daily tipping-bucket rainfall amounts between 1.0 and 2.5 in. were corrected by a factor of 1.11, and daily rainfall amounts totaling more than 2.5 in. were corrected by a factor of 1.14. Daily rainfall amounts of more than 1.0 in. between December and April were overcorrected, probably because winter rains are generally less intense than summer thundershowers. During this period, the daily rainfall was corrected instead by a factor of 1.04. Weekly sums from the corrected data compared well with weekly rainfall totals measured in the storage rain gage (fig. 18). The mean difference was 0.03 in., and the largest deviation between the data from the storage rain gage and the corrected weekly tipping-bucket precipitation total was 0.19 in. out of a total weekly rainfall of 2.21 in. (8.6 percent error).

Daily tipping-bucket data are missing for several weeks in November 1989 when the storage module failed at the land-based climate station and for several days in December 1989 when the gage malfunctioned during a period when temperatures remained below freezing. Rainfall from the weighing-bucket rain gage was used as backup for periods of missing record. The weighing-bucket rain gage read slightly low during this period, prior to a recalibration of the gage. Thus, a regression equation (table 5) was used to estimate the missing daily rainfall data from the weighing-bucket rain-gage data.

Monthly rainfall at Lake Barco for the period between May 1989 and December 1990 varied from a maximum of 9.93 in. in June 1990 to a minimum of 0.94 in. in October 1989 (fig. 19). Total rainfall between May 1989 and December 1989 was 28.39 in., which is a 10.66-in. deficit compared to the 30-year mean (1951-1980) of 39.05 in. for these months at the NOAA 3WSW site at Gainesville (National Oceanic and Atmospheric Administration, 1988). Rainfall was also deficient in 1990. The annual total of 43.73 in. for 1990 was 9.11 in. lower than the annual 30-year mean of 52.84 in. at Gainesville. Much of the rainfall deficit occurred during the typically wet summer months of July through September (fig. 19). Eleven of the 20 months of data collection had rainfall that was more than 1.0 in. below the monthly long-term mean at Gainesville. Only 2 months (June and October 1990) had rainfall that exceeded the mean monthly rainfall at Gainesville by 1.0 in. or more.

Table 5. Summary of regressions used to estimate missing data

[R^2, coefficient of determination; °C, degrees Celsius; mb, millibars; (cal/cm^2)/d, calories per square centimeter per day; (Ei/m^2)/d, Einsteins per square meter per day; (mJ/m^2)/d, millijoules per square meter per day; mi/h, miles per hours; in., inch; ft, foot; N/A, not applicable]

Estimated variable	Independent variable	R^2	Standard error (in units of estimated variable)	Number of observations	Percent of record estimated
Water-surface temperature (°C)	Top thermocouple temperature (°C)	0.995	0.402	462	24.6
Vapor pressure difference[1] (mb)	Julian day	.72	.911	49	54.9
Vapor pressure (mb)	Vapor pressure from old raft relative humidity sensor[2] (mb)	.85	.453	24	13.7
Vapor pressure (mb)	Vapor pressure from new raft relative humidity sensor[2] (mb)	.99	.726	115	8.6
Longwave radiation (cal/cm^2)/d	Natural log of vapor pressure	.93	24.5	591	3.3
Shortwave radiation (cal/cm^2)/d	Photosynthetically active radiation[3] (Ei/m^2)/d	.83	57.0	31	1.1
Shortwave radiation (cal/cm^2)/d	Total radiation[3] (mJ/m^2)/d	.49	85.0	64	2.1
Windspeed at raft station (mi/h)	Windspeed at land station (mi/h)	.43	.935	407	30.3
Daily rainfall (in.)	Daily weighing rainfall (in.)	.995	.030	82	3.3
Mean temperature from thermal survey measurements at:	Daily mean temperature from thermocouple at:				
5-ft depth (°C)	5-ft depth (°C)	.992	.507	76	N/A
10-ft depth (°C)	10-ft depth (°C)	.994	.436	76	N/A
Lake Goodson stage (feet above sea level)	Lake Barco stage (feet above sea level)	.998	.038	55	N/A
Long Lake stage (feet above sea level)	Lake Barco stage (feet above sea level)	.997	.047	61	N/A
Lake Rowan stage (feet above sea level)	Lake Barco stage (feet above sea level)	.988	.105	62	N/A
Head in well WTB-5 (feet above sea level)	Head in well WTB-6 (feet above sea level)	1.00	.029	46	N/A
Head in well WTB-7 (feet above sea level)	Head in well WRB-9 (feet above sea level)	.997	.106	33	N/A
Head in well WTB-13 (feet above sea level)	Head in well WTB-12 (feet above sea level)	.995	.089	23	N/A
Head in well WTB-18 (feet above sea level)	Head in well IPNB-20 (feet above sea level)	1.00	.024	19	N/A
Head in well WTB-20 (feet above sea level)	Head in well IPNB-20 (feet above sea level)	.998	.053	36	N/A
Head in well WTB-22 (feet above sea level)	Lake Barco stage (feet above sea level)	.997	.054	19	N/A

[1]Vapor pressure measured with the raft relative humidity sensor was corrected by subtracting the vapor pressure difference (fig. 17).

[2]Raft relative humidity sensor replaced in July 1990.

[3]Data from J.M. Mishoe, University of Florida, written commun., 1990.

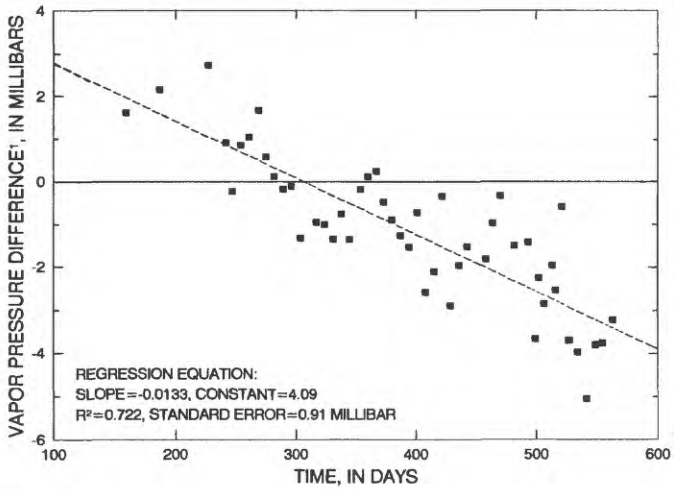

Figure 17. Difference between vapor pressure calculated from relative-humidity sensor and that calculated from ventilated psychrometer plotted against time. (Vapor pressure calculated from the raft relative-humidity sensor was corrected by subtracting the vapor pressure difference derived from the regression equation.)

Lake Storage

The stage of Lake Barco dropped throughout most of the period of record (fig. 20). The lake level declined almost 7 ft, from a high of 88.02 ft above sea level in December 1988 to 81.19 ft above sea level by the end of the period of record (January 1, 1991). Lower than normal summer rainfall in 1989 and 1990 resulted in little or no increase in stage during the normal wet season. Stage-volume and stage-area relations compiled from the lake bathymetry are shown in figure 21. Lake volume was reduced by about 45 percent between December 1988 and early January 1991, from 1.75×10^7 to 0.95×10^7 ft^3.

Ground Water

Information about the hydraulic head distribution around Lake Barco aids in understanding the interaction of the lake with the ground-water flow system. Quantification of ground-water flux rates is planned for presentation in a future report.

Areal Head Distribution

Water levels in the wells near Lake Barco showed declines similar to the decline in lake stage during the period of record. Hydrographs for representative water-table wells are shown in figure 22. When monitoring first began in late September 1988, the water table around a large area of the lake was higher than the lake stage, indicating a large area of ground-water inflow. This high level of the water table was probably the result of higher than normal rainfall in August and September 1988. According to NOAA records, 26.04 in. of rain fell in Gainesville in August and September 1988 (12.45 in. in excess of the mean for these months). Similarly high rainfall totals were reported near Lake Barco during these months (R. Franz, University of Florida, written commun., 1991). Maps of the water-table in the surficial aquifer for December 1988 and April 1990 are shown in figure 23.

By May 1989, the water table remained higher than the lake around the northeastern perimeter, but the water table to the north and northwest of the lake was depressed to just below the lake level. This water-table configuration remained for the rest of the monitoring period, and the area of ground-water inflow was limited to approximately 12 percent of the total lake circumference (fig. 23). The high level of the water table similar to that observed in September 1988 did not follow the summer rainy season in 1989 or 1990 probably because of below average recharge. Rainfall between May and September 1989 and 1990 was approximately 8 in. below normal during both years. The high in the water table throughout the period was in the northern part of the Lake Barco drainage basin.

The water table was lower than the lake along its entire southern perimeter after September 1988, indicating leakage from the lake in this area. The steepest head gradients were on the southeastern side of the lake where the water table generally was 3 ft below the lake stage. In addition, the water

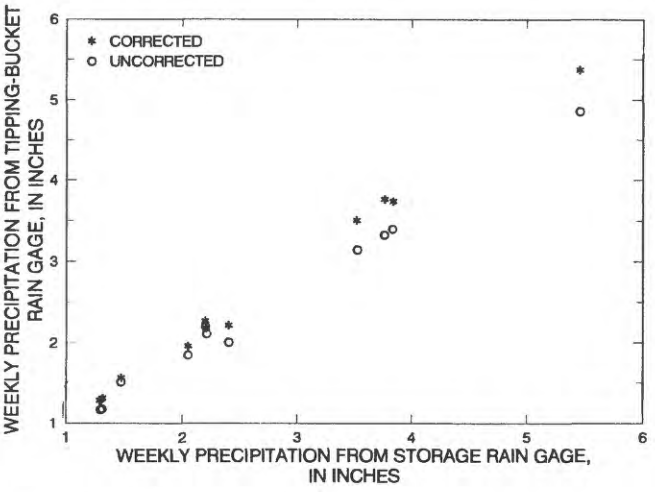

Figure 18. Uncorrected and volume-corrected cumulative weekly precipitation greater than 1.0 inch measured by the tipping-bucket rain gage plotted against weekly precipitation from the storage rain gage. (Daily rainfall totals between 1.0 and 2.5 inches were adjusted by a factor of 1.04 for the months of December through April and by a factor of 1.11 for the months of May through November; daily rainfall totals greater than 2.5 inches were adjusted by a factor of 1.14.)

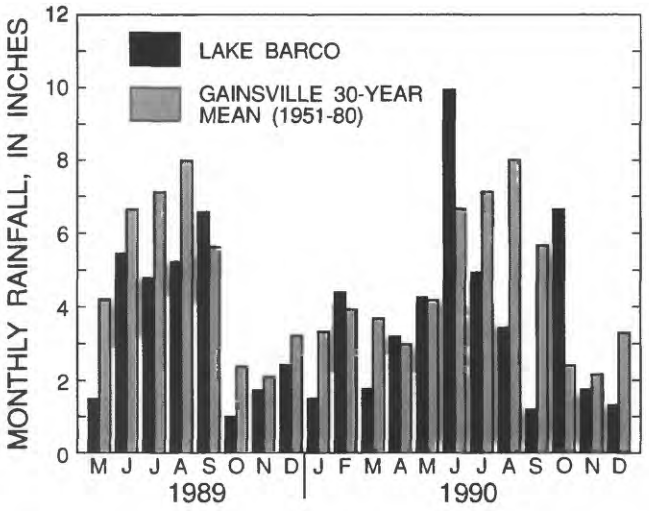

Figure 19. Monthly rainfall at Lake Barco and the 30-year meam at Gainesville.

table to the south of Lake Barco was lower than the stages of nearby Lake Goodson and Long Lake (fig. 23). This trough in the water table was much more pronounced during the period of drought. Limited data are available for periods of high recharge, but a more lateral flow component from Lake Barco to Lake Goodson is probably present during these periods. A depression also occurred in the water table between Lake Barco and Lake Rowan for much of the period of record.

The stages of Lake Goodson and Long Lake were approximately equal to each other and were generally 2 ft lower than the stage of Lake Barco. The stage of Lake Rowan was generally less than 1 ft lower than the stage of Lake Barco. Like Lake Barco and the intervening water table, the levels of these lakes also declined during the period of record (fig. 24). There were good correlations between the stage of Lake Barco and the stages of the surrounding lakes (table 5).

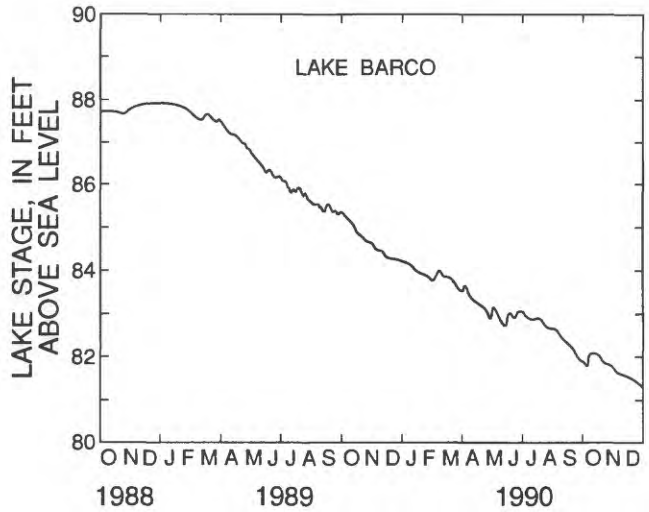

Figure 20. Stage of Lake Barco for the period of record.

Vertical Head Distribution

A distinct decrease in head with depth, indicative of recharge, was observed in each of the three well nests (fig. 25). At 1PNB, the head difference between the water table and the Upper Floridan aquifer was generally 5 ft. Most of the head loss (approximately 3.5 ft) occurred between depths of 80 and 110 ft (wells 1PNB-80 and 1PNB-FL) within the Hawthorn Group. At 2PNB, the head difference between the water table and the Upper Floridan aquifer was only 2 ft because of the lower altitude of the water table. This difference in vertical hydraulic gradients is probably due at least in part to differences in confining units at the two sites. At 1PNB, a clay-rich bed is present in the lower Hawthorn Group immediately above the contact with the limestone of the Upper Floridan aquifer. This clay-rich bed appears to be missing at 2PNB where, instead, a massive sandbed occurs immediately above the limestone. The sands at 2PNB should enhance vertical leakage from the lower parts of the surficial aquifer system to the Upper Floridan aquifer, whereas at 1PNB, the clay-rich beds form a semiconfining layer overlying the Upper Floridan aquifer.

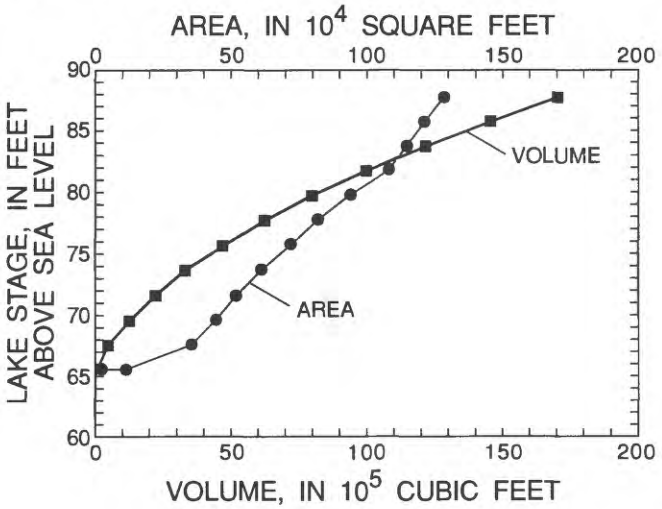

Figure 21. Stage-volume and stage-area relations for Lake Barco.

The water levels in the midlake wells were generally equal to the lake level (or within the measurement accuracy of 0.05 ft). Midlake well 4 (MLW-4) was the only well with a measurable head difference, which generally was 0.1 ft lower than the lake stage. The wells were checked and resealed at all joints to ascertain there were no leaks in the casings. Lake sediments also appeared to be tightly sealed around the casing at the sediment-water interface; however, preferential flow near the casing is possible. Provided the readings are accurate, the equal heads may be the result of a good hydraulic connection between the lake and the uppermost part of the surficial aquifer system, implying that lake-sediment permeability is not limiting leakage. Otherwise, a much greater head gradient would be expected between the lake and the aquifer below the lake.

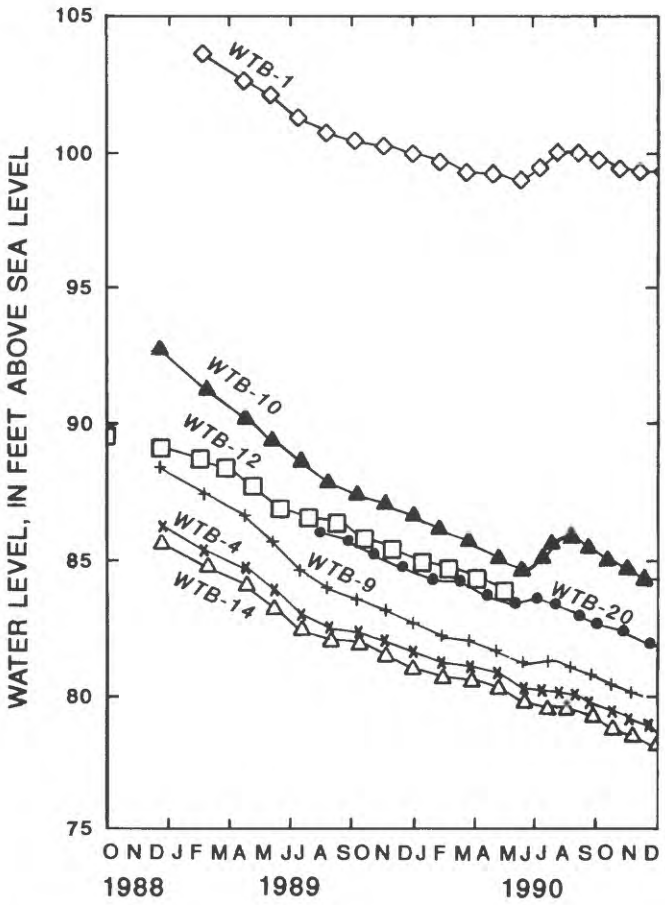

Figure 22. Water levels in selected water-table wells near Lake Barco.

The vertical head distribution around Lake Barco is shown along a cross section through the basin in figure 26. Hydraulic heads on the northern side of the lake are always greater than heads at corresponding altitudes on the southern side of the lake. Before May 1989, ground water flowing from the northern part of the basin along transect *A-A′* was intercepted by the lake, as indicated by a higher head at well 1PNB-20, 88.44 ft, than the lake stage, 88.02 ft (fig. 26). After May 1989, ground water that moved laterally toward the lake from the northern half of the basin was not intercepted by the lake along this transect. Instead, water flows under the lake along transect *A-A′*, and the sublake flow may be augmented by leakage through the lake bottom (fig. 26). Along the northeastern part of the lake perimeter where the water table is higher than the lake, ground-water inflow occurs. Because vertical head gradients in this area are not known, the depth to which inflow occurs along the lake bottom cannot be inferred.

Ground Water and Lake Interactions

Lake Barco can be described as a flow-through type lake with respect to the surficial aquifer system because it receives ground-water inflow on the northern perimeter of the lake and loses water to the aquifer along the southern perimeter. Shallow ground-water flow within the northern half of the basin is toward the lake (fig. 23). Ground-water inflow, however, occurred only on the northeastern margin of the lake during most of the period of study. Water-table gradients toward Lake Barco were probably well below normal during most of the study, as rainfall, and thus recharge to the surficial aquifer system, was well below normal. Following periods of high recharge (such as in September 1988), the water-table configuration around the lake probably is considerably different, and the amount of ground-water inflow to the lake may be substantially greater than during a drought year.

The head distribution to the south of the lake implies that ground-water flow from Lake Barco and Lake Goodson converges toward the water-table depression between the lakes. This water then moves downward to the Upper Floridan aquifer. The strong vertical gradient, which may be enhanced by local geologic conditions, interrupts the more likely horizontal flow pattern from the higher elevation lake (Lake Barco) to the lower elevation lakes (Lake Goodson and Long Lake). This trough in the water table also may be the result of slower recharge to the water table because of higher clay content in the 20 ft of unsaturated zone in the southern part of the basin. This condition was probably exacerbated by low recharge during the study period because of the drought. During periods of high recharge, a lateral flow component probably exists between Lake Barco and Lake Goodson.

The absence of a symmetrical pattern of ground-water inflow along the northern margin of the lake, as well as the steep outflow gradients to the south of the lake, may be explained by nonuniform geology beneath and immediately around the lake. Irregular solution features in the limestone beneath Lake Barco may cause significant variations in the depth to the top of the limestone. This in turn may influence the degree of hydraulic connection between the surficial aquifer system and Upper Floridan aquifer beneath the lake.

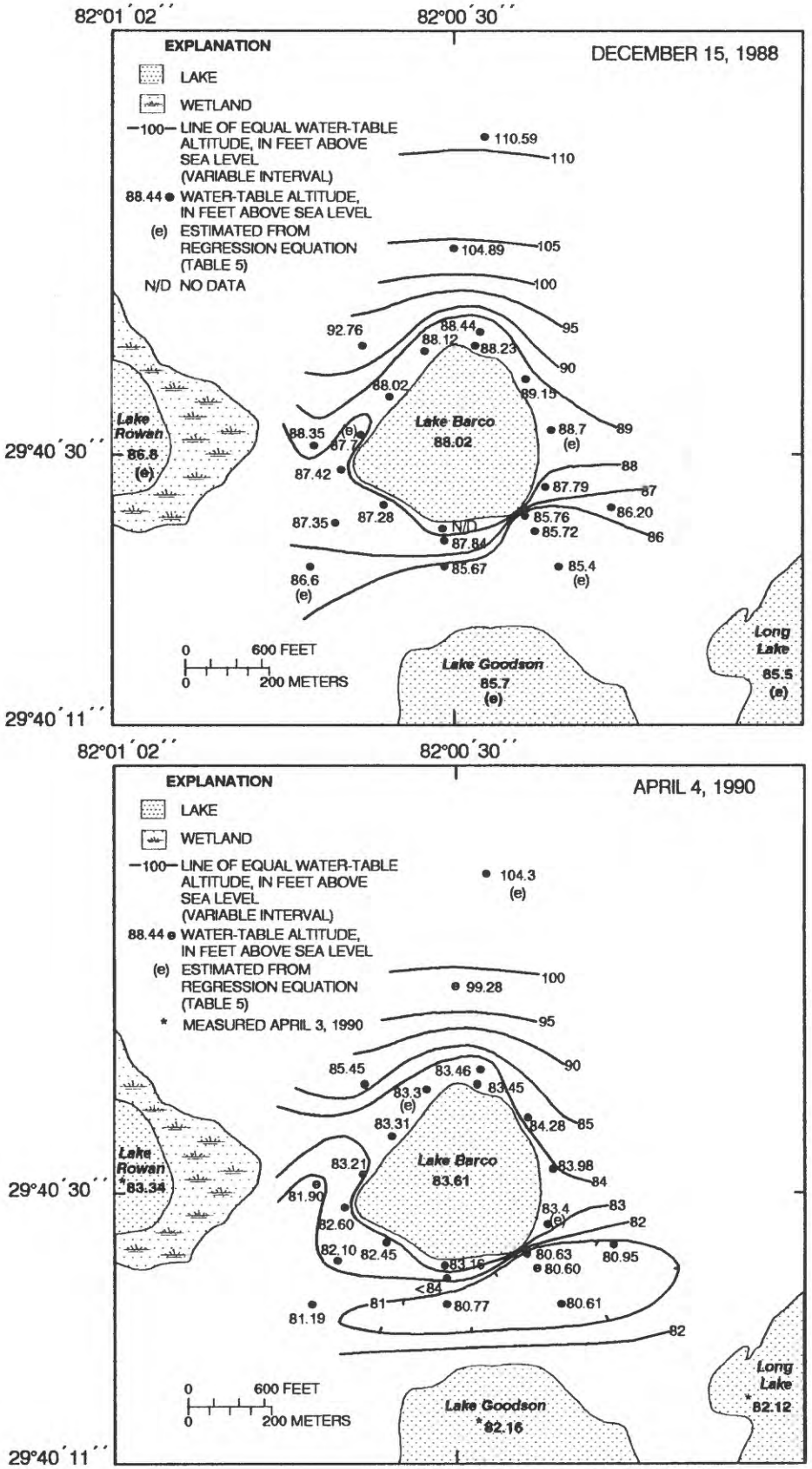

Figure 23. Configuration of the water table near Lake Barco for December 15, 1988, and April 4, 1990.

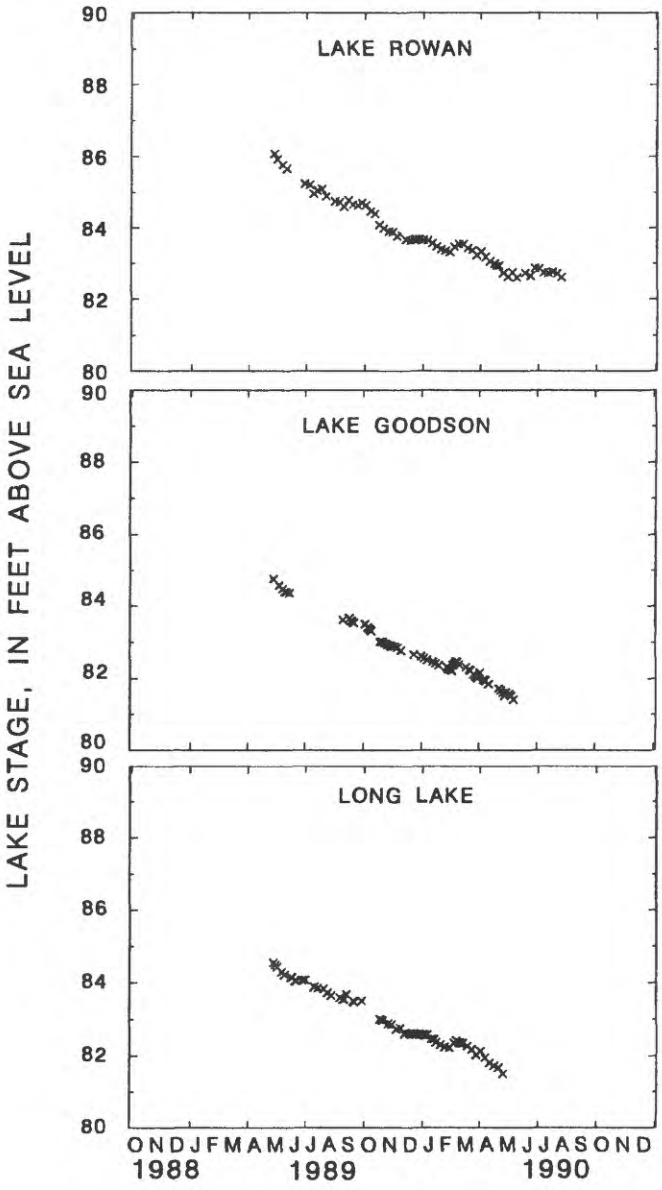

Figure 24. Stages of Lake Rowan, Lake Goodson, and Long Lake.

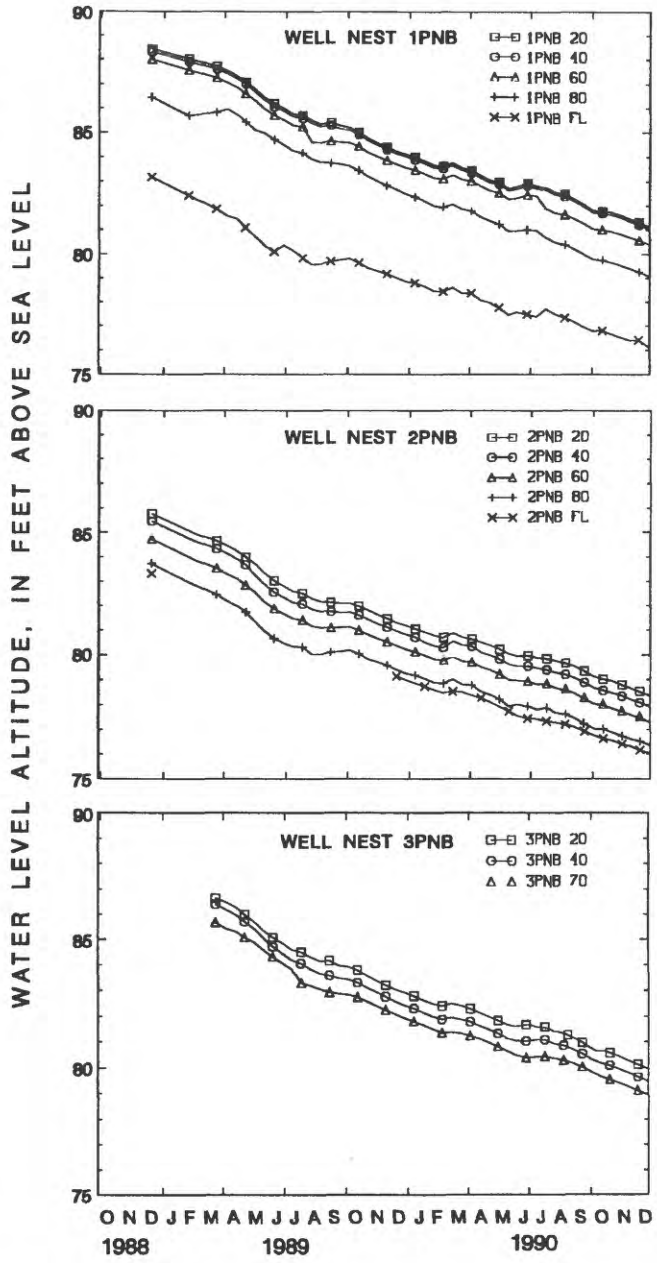

Figure 25. Water levels in wells finished at different depths at well nests 1PNB, 2PNB, and 3PNB.

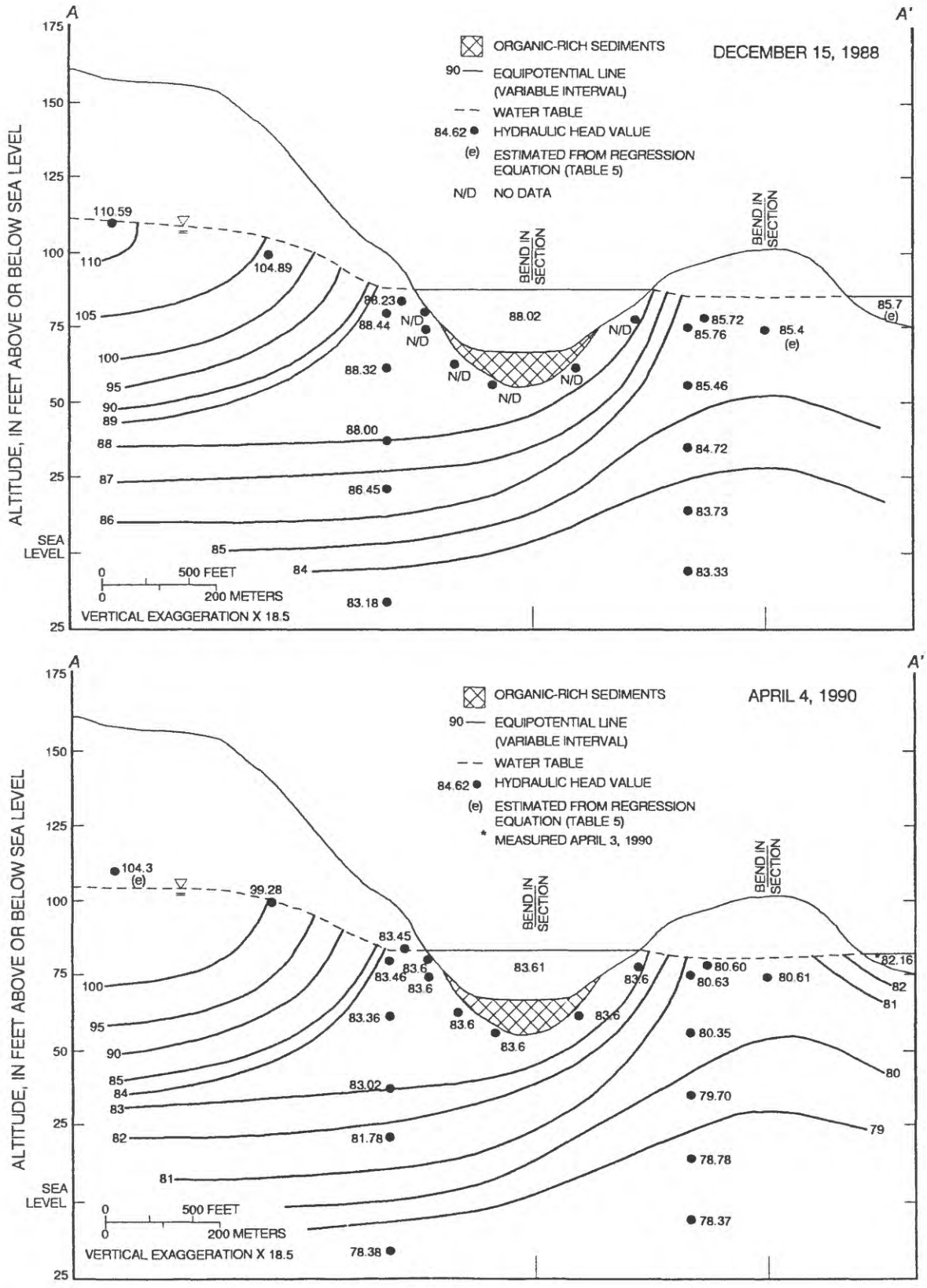

Figure 26. Cross section through Lake Barco showing vertical head distribution near the lake for December 15, 1988, and April 4, 1990. (Location of section is shown in fig. 5. The head distribution under the lake is inferred from measurements in midlake wells. If these head measurements are not representative, more head loss would be expected through the lake sediments.)

SUMMARY

A study is underway to quantify the hydrologic budget of Lake Barco, a clear water, acidic seepage lake in north-central Florida. By understanding the hydrologic budget, particularly the ground-water flux, an assessment can be made of the relative importance of hydrologic pathways in controlling the solute budget and acid neutralizing capacity of the lake. The surface area of Lake Barco is 29 acres, and mean depth is 13 ft. No development has occurred within the drainage basin of the lake.

The basin is underlain by 100 to 150 ft of unconsolidated sands and clays. The surficial aquifer system occurs within undifferentiated surficial deposits that are 33 to 53 ft thick near Lake Barco. The Hawthorn Group semiconfines the surficial aquifer system from the Upper Floridan aquifer. Near the lake, the Hawthorn Group generally consists of phosphatic, poorly sorted, sandy clays to clayey sands and gravels. The contact with limestones of the Ocala Group is irregular near Lake Barco and occurs between 3 and 46 ft below sea level at three nested well sites. The depth to the limestone beneath the lake, delineated using seismic reflection, also was quite irregular. The solution feature, or features, responsible for the formation of the lake probably occurs within the center of the lake where the seismic signal was obscured because of thick accumulations of organic-rich sediments. The lake is probably a sinkhole that is at least 1,000 years old.

The basin was instrumented for hydrologic and climatologic data collection to compute the hydrologic budget of the lake. Data were collected to estimate water gains (precipitation and ground-water inflow) and losses (evaporation and leakage to ground water) and change in lake storage. Climatologic data were collected to calculate evaporation using the energy-budget and mass-transfer methods, and vertical and areal head distributions were monitored in a network of observation wells. Monitoring of lake stage and ground-water heads began in September 1988; precipitation and climatologic monitoring began in May 1989. Data through December 1990 are included in this report.

Many of the climatologic parameters varied significantly between the cooler, drier winter months and the warm, rainy summer months. Daily mean lake temperature ranged from 8.9 to 32.8°C, and daily mean air temperature ranged from -4.0 to 30.0°C. The lake does not thermally stratify, and daily mean lake temperature generally varied by less than 1°C from the surface to the bottom of the lake. Daily mean vapor pressure ranged from 4.4 to 32.0 mb. Rainfall during the 20-month period of data collection (May 1989-December 1990) was 72.12 in., almost 20 in. below the long-term mean at Gainesville. As a result of deficit rainfall, lake stage declined from a high of 88.02 ft above sea level in December 1988 to a low of 81.19 ft above sea level on January 1, 1991. Lake volume was reduced by 45 percent during this period.

Ground-water heads declined during the period of record. The water table is highest in the northern part of the basin and is lowest south of the lake. Around the northeastern side of the lake, the water table immediately adjacent to the lake was higher than lake stage. For most of the period of study, the water table was depressed slightly below lake stage around the northern and northwestern edge of the lake. The water table was higher than the lake stage in this area during the fall and early winter of 1988 following a period of high recharge. South of the lake, the water table slopes away from the lake, with the steepest gradients on the southeastern side of the lake.

Lake Barco is a flow-through lake with respect to the surficial aquifer system. Ground water enters the lake primarily on its northeastern side, and the lake loses water to the aquifer along its southern side. In addition, leakage may occur over a large part of the lakebed. Hydraulic head decreases with depth, indicating recharge from the surficial aquifer system to the Upper Floridan aquifer. Heads on the northern side of the lake are greater than heads at corresponding altitudes on the southern side of the lake. These lower head values in the southern part of the basin may be controlled by a better hydraulic connection between the surficial aquifer system and the Upper Floridan aquifer. In addition, higher clay content in the unsaturated zone in the southern part of the basin may limit recharge to the water table. Irregular ground-water flow patterns are probably controlled by nonuniform geology associated with the karst terrain.

REFERENCES

Anderson, E.R., 1954, Energy-budget studies, *in* Water loss investigations—Lake Hefner studies, technical report: U.S. Geological Survey Professional Paper 269, p. 71-119.

Anderson, E.R., Anderson, L.J., and Marciano, J.J., 1950, A review of evaporation theory and development of instrumentation: U.S. Navy Electronics Laboratory Report 159, 71 p.

Arrington, D.V., and Lindquist, R.C., 1987, Thickly mantled karst of the Interlachen area, *in* Beck, B.F., and Wilson, W.L., eds., Proceedings of Second Multidisciplinary Conference on Sinkholes and the Environmental Impacts of Karst: Orlando, Florida Sinkhole Research Institute, p. 31-39.

Aucott, W.R., 1988, Areal variation in recharge to and discharge from the Floridan aquifer system in Florida: U.S. Geological Survey Water-Resources Investigations Report 88-4057, 1 sheet.

Baker, L.A., and Brezonik, P.L., 1988, Dynamic model of in-lake alkalinity generation: Water Resources Research, v. 24, no. 1, p. 64-74.

Baker, L.A., Pollman, C.D, and Eilers, J.M., 1988, Alkalinity regulation in softwater Florida lakes: Water Resources Research, v. 24, no. 7, p. 1069-1082.

Bear, Jacob, 1979, Hydraulics of groundwater: New York, McGraw-Hill, p. 83-169.

Beck, B.F., and Wilson, W.L., 1988, Interpretation of ground penetrating radar profiles in karst terrane: Second Conference on Environmental Problems in Karst Terranes and Their Solutions, Proceedings: Dublin, Ohio, National Water Well Association, p. 347-367.

Bermes, B.J, Leve, G.W., and Tarver, G.R., 1963, Geology and ground-water resources of Flagler, Putnam, and St. Johns Counties, Florida: Florida Geological Survey Report of Investigations no. 32, 97 p.

Brooks, H.K., 1981, Physiographic divisions of Florida: Gainesville, Center for Environmental and Natural Resources, University of Florida.

Eilers, J.M, Landers, D.H., and Brakke, D.F., 1988, Chemical characteristics of lakes in the southeastern United States: Environmental Science Technology, v. 22, no. 2, p. 172-177.

Ficke, J.F., 1972, Comparison of evaporation computation methods, Pretty Lake, Lagrange County, northeastern Indiana: U.S. Geological Survey Professional Paper 686-A, 48 p.

Franz, R., and Hall, D.W., 1990, Vegetative communities and annotated plant lists for the Katharine Ordway Preserve-Swisher Memorial Sanctuary, Putnam County, Florida (1985-1989): Gainesville, Florida Museum of Natural History, University of Florida, Ordway Preserve Research Series Report no. 3, 94 p.

Harbeck, G.E., Jr., 1962, A practical field technique for measuring reservoir evaporation utilizing mass-transfer theory: U.S. Geological Survey Professional Paper 272-E, p. 101-105.

Landers, D.H., Overton, W.S., Linthurst, R.A., Brakke, D.F., 1988, Eastern lake survey, regional estimates of lake chemistry: Environmental Science Technology, v. 22, no. 2, p. 128-135.

Lane, E., 1986, Karst in Florida: Florida Geological Survey Special Publication no. 29, 100 p.

Lee, T.M., Adams, D.B. Tihansky, A.B., and Swancar, Amy, 1991, Methods, instrumentation, and preliminary evaluation of data for the hydrologic budget assessment of Lake Lucerne, Polk County, Florida: U.S. Geological Survey Water-Resources Investigations Report 90-4111, 42 p.

Locker, S.D., Brooks, G.R., and Doyle, L.J., 1988, Results of a seismic reflection investigation and hydrogeologic implications for Lake Apopka, Florida: Center for Nearshore Marine Science final report to St. Johns River Water Management District, 39 p.

McDonald, M.G, and Harbaugh, A.W., 1988, A modular three-dimensional finite-difference ground-water flow model: U.S. Geological Survey Techniques of Water-Resources Investigations, book 6, chap. A1 [variously paged].

McQuillan, R., and Ardus, D.A., 1977, Exploring the geology of shelf seas: Houston, Gulf Publishing Company, 234 p.

Miller, J.A., 1986, Hydrogeologic framework of the Floridan aquifer system in Florida and parts of Georgia, Alabama, and South Carolina, Regional Aquifer System Analysis: U.S. Geological Survey Professional Paper 1403-B, 91 p.

National Oceanic and Atmospheric Administration, 1988, Climatological data annual summary, Florida, 1988: Asheville, N.C., v. 92, no. 13.

Pollman, C.D., Lee, T.M., Andrews, W.J., Sacks, L.A., Gherini, S.A., and Munson, R.K., Preliminary analysis of the hydrologic and geochemical controls on acid-neutralizing capacity of two acidic seepage lakes in Florida: Water Resources Research, v. 27, no. 9, p. 2321-2335.

Puri, H.S., 1957, Stratigraphy and zonation of the Ocala Group: Florida Geological Survey Bulletin no. 38, 248 p.

Reik, B.A., 1982, Clay mineralogy of the Hawthorn Formation in northern and eastern Florida, *in* Scott, T.M., and Upchurch, S.B., eds., Miocene of the southeastern United States, Proceedings of a Symposium: Florida Bureau of Geology Special Publication no. 25, p. 247-250.

Scott, T.M., 1983, The Hawthorn Formation of northeastern Florida, part I, The geology of the Hawthorn Formation of northeastern Florida: Florida Bureau of Geology Report of Investigations no. 94, 35 p.

——— 1988, The lithostratigraphy of the Hawthorn group (Miocene) of Florida: Florida Geological Survey Bulletin no. 59, 148 p.

Sheriff, R.E., 1980, Seismic stratigraphy: Boston, IMRDC Publishing Company, 227 p.

Sinclair, W.C., and Stewart, J.W., 1985, Sinkhole type, development, and distribution in Florida: Florida Bureau of Geology Map Series no. 110, 1 sheet.

Snyder, S.W., Evans, M.W., Hine, A.C., and Compton, J.S., 1989, Seismic expression of solution collapse features from the Florida Platform, *in* Beck, B.F., ed., Proceedings of Third Multidisciplinary Conference on Sinkholes and the Engineering and Environmental Impacts of Karst: Orlando, Florida Sinkhole Research Institute, p. 281-298.

Southeastern Geological Society, 1986, Hydrogeological units of Florida: Florida Bureau of Geology Special Publication no. 8, 8 p.

Stewart, J.W., 1980, Areas of natural recharge to the Floridan aquifer in Florida: Florida Bureau of Geology Map Series no. 98, 1 sheet.

Sturrock, A.M., Jr., 1985, Instrumentation for measuring lake and reservoir evaporation by the energy-budget and mass-transfer methods: U.S. Geological Survey Open-File Report 84-863, 21 p.

Wentz, D.A., Garrison, P.J. Garrison, and Bockheim, J.G., 1989, Chemical input-output budgets, *in* Knauer, D., and Brouwer, S.A., eds., The Wisconsin regional integrated lake acidification study (RILWAS), 1981-1983: Palo Alto, Calif., Electric Power Research Institute EPRI EA-6214, p. 7-1 through 7-30.

Winter, T.C., 1976, Numerical simulation of the interaction of lakes and ground water: U.S. Geological Survey Professional Paper 1001, 44 p.

——— 1981, Uncertainties in estimating the water balance of lakes: Water Resources Bulletin, v. 17, no. 1, p. 82-115.

Yobbi, D.K., and Chappell, G.C., 1979, Summary of the hydrology of the Upper Etonia Creek basin: St. Johns River Water Management District Technical Publication SJ 79-5, 67 p.

*U.S. Government Printing Office: 1993 — 733-120/80011